2021

# Characterization of CD45+ Primary Fibroblasts in Interstitial Lung Disease

Charles Ford Reese III
*Medical University of South Carolina*

Characterization of CD45+ Primary Fibroblasts in Interstitial Lung Disease by

Charles Ford Reese III

A dissertation submitted to the faculty of the Medical University of South Carolina in partial fulfillment of the requirements for the degree of Doctor of Philosophy in the College of Graduate Studies.

Division of Rheumatology and Immunology

2021

Approved by:

| | |
|---|---|
| Chairman, advisory committee | Stanley Hoffman |
| | Dhandapani Kuppuswamy |
| | Carole Wilson |
| | Roger Markwald |
| | Richard Silver |

**Table of Contents**

## List of Tables

**List of Figures**

**Key to Abbreviations**

| | |
|---|---|
| α-sma | Alpha Smooth Muscle Actin |
| BAL | Bronchoalveolar Lavage |
| BM | Bone Marrow |
| Col I | Collagen Iα1 |
| CSD | Caveolin Scaffolding Domain |
| ECM | Extracellular Matrix |
| EGFP | Enhanced Green Fluorescent Protein |
| FMO | Fluorescence Minus One |
| HSP47 | Heat Shock Protein 47 |
| ILD | Interstitial Lung Disease |
| IP | Intraperitoneal |
| MFI | Mean Fluorescent Intensity |
| MSCs | Mesenchymal Stem Cells |
| PCA | Principal Component Analysis |
| PH | Pulmonary Hypertension |
| SSc | Systemic Sclerosis |
| UMAP | Uniform Manifold Approximation and Projection |

WCSD Water Soluble Caveolin Scaffolding Domain

Charles Ford Reese III. Characterization of CD45+ Fibroblasts in Interstitial Lung Disease. (Under the direction of Stanley Hoffman)

Abstract

The role of cells of the hematopoietic lineage in fibrosis associated with interstitial lung disease (ILD) is controversial; whether monocytes solely differentiate into macrophages that activate resident fibroblasts, or if they can also differentiate into fibrocytes (CD45+/Col I+ cells) that then differentiate into fibroblasts has been debated. By using systemic bleomycin to induce fibrosis in a bone marrow transplant and transgenic mouse models, as well as using human lung tissue from a patient with scleroderma-associated ILD, we studied the contribution of the hematopoietic lineage to the fibroblast population using flow cytometry and single cell RNA sequencing. Further, our studies revealed reasons why fibrocytes are lost when fibroblast cultures are passaged. Finally, we evaluated how treatment of mice with a novel, water-soluble version of caveolin scaffolding domain (CSD) called WCSD affects fibrocyte accumulation and fibrosis in our animal model. We found that during fibrosis, fibrocytes increase in number and in their expression of Col I both in the lung tissue and in the bronchiolar lavage fluid (BAL). The appearance of Col I in CD45+ precursors occurs after their recruitment into the lung. Interestingly, fibrocytes express higher levels of monocyte/macrophage markers (CD45, CD16, CD68, CD206) than do CD45+/Col I- cells. In vitro experiments demonstrated that CD45+/Col I+ cells are at first predominant in fibroblast cultures, but then are lost progressively during passage. Furthermore, these fibrocytes do not appear to grow in vitro in the absence of CD45-/Col I+ fibroblasts.

Treating mice with WCSD inhibited fibrocyte accumulation as well as overall collagen I, Tenascin C, α-sma, and HSP47 levels and vascular leakage. The decreased fibrocyte accumulation may result both from decreased precursor recruitment due at least in part to decreased vascular permeability and from decreased differentiation of fibrocytes from CD45+/Col I- precursor monocytes. In summary, CD45+ cells accumulate in lung tissue during fibrosis and contribute to pathological remodeling by differentiating into myofibroblasts that overexpress ECM proteins and myofibroblast markers. Their contribution to fibrosis can be inhibited by WCSD which serves as a surrogate for caveolin-1, a protein known to be reduced in expression in multiple cell types from patients with fibrotic lung disease.

## Introduction

Fibrosis is a common underlying factor in many different diseases. In the Western world, diseases with a fibrotic component are responsible for nearly 45% of deaths (Wynn 2004). Indeed, fibrosis occurs in all the main organ systems, including the heart, kidney, lung, liver, and skin (Masuda, Fukumoto et al. 1994, Sunamoto, Kuze et al. 1998, Fischer and Du Bois 2012). When an injury or disease occurs, a series of cellular and molecular processes begins that ultimately may result in tissue fibrosis. This is an adaptive response that helps to close and repair wounds (Xie, Wang et al. 2018), and is initially a beneficial process. However, if the fibrotic response occurs for an extended period of time, it can become pathogenic and lead to excessive deposition of extra cellular matrix (ECM) proteins, scarring, and loss of organ function that can ultimately result in organ failure and death.

The fibrotic response to injury occurs in several stages (Wynn 2004, Rockey, Bell et al. 2015). The initiation of fibrosis begins when an injury occurs to the tissue. After injury, resident effector cells become activated and drive a series of processes that result in the recruitment of various cell types (i.e., monocytes, macrophages, neutrophils, T lymphocytes, and B lymphocytes), as well as tissue repair and replacement of damaged and injured cells. The recruitment of inflammatory cells into the site of injury activates fibroblasts/myofibroblasts to inappropriately deposit high levels of ECM proteins into the tissue, ultimately leading to loss of organ function and fibrosis.

Interstitial lung disease (ILD), also called interstitial lung pneumonias, is a term used to represent a large group of fibrotic diseases that occur in the lung. There are a

variety of stimuli that can lead to ILD including toxins, radiation, infections, and autoimmune disorders (such as in systemic sclerosis/scleroderma (SSc)). ILD can also occur idiopathically (Borchers, Chang et al. 2011). These diseases are characterized by injury to alveolar epithelial cells, excessive recruitment of inflammatory cells, activation and proliferation of fibroblast/myofibroblasts, over production of ECM, and hyperplasia of fibroblasts and type II pneumocytes (Selman and Pardo 2002, Wang 2009).

Two of the more devastating forms of ILD are idiopathic pulmonary fibrosis (IPF) and SSc related ILD, both of which are often fatal and carry a worse prognosis than many cancers. More specifically, SSc is a systemic autoimmune disease that can involve nearly every organ system in the body, and is characterized by dysfunction of endothelial and fibroblast cells, small vessel vasculopathy, and the excessive production and deposition of ECM proteins. Despite the fact that the disease can involve most organ systems, disease progression to the lung is the leading cause of death for patients with SSc (Solomon, Olson et al. 2013). Lung involvement can result in both ILD and pulmonary hypertension (PH). PH is characterized by high blood pressure in the lung and right side of the heart resulting from injuries to the vascular endothelium, and an increased inflammatory response leading to ablation and narrowing of pulmonary arteries (Solomon, Olson et al. 2013, Vonk Noordegraaf, Groeneveldt et al. 2016). Until recently, there were no FDA approved treatments for these diseases. Two drugs, pirfenidone and nintedanib, have since gained FDA approval for patients with IPF, and nintedanib was approved recently for patients with SSc. Both appear to be modestly effective in slowing

disease progression (Daccord and Maher 2016). However, the prognosis for patients is still poor.

To study ILD, a variety of different animal models have been used to try and best recreate the features of the disease in humans. Some of these methods include exposure to insults such as bleomycin, cigarette smoke, fluorescein isothiocyanate, and silica (Lee, Reese et al. 2014). The most commonly used model for ILD is treatment with the antitumor antibiotic, bleomycin (Moeller, Ask et al. 2008, Mouratis and Aidinis 2011). Originally discovered in 1962, bleomycin received FDA approval in 1973 for the treatment of various squamous cell carcinomas, but the drug has been limited in its usefulness due to its potential to cause pulmonary fibrosis. Researchers have taken advantage of this side effect and deliver bleomycin to rodents to induce pulmonary fibrosis by a variety of methods. Administration of bleomycin is done either directly (intratracheal or intraoral delivery), or systemically (intravenous, intraperitoneal, subcutaneous, or through osmotic pump delivery) (Harrison Jr and Lazo 1987, Moore and Hogaboam 2008, Aono, Ledford et al. 2012, Lee, Reese et al. 2014).

Historically, the cells that overexpress collagen in many fibrotic diseases, such as ILD, were believed to be resident fibroblasts that have been activated through the release of various cytokines. Once activated, the fibroblasts become myofibroblasts that overexpress collagen and cause fibrosis. However, recent evidence suggests that some fibroblast precursors are not resident fibroblasts. Rather, they may originate in the bone marrow (BM) and are recruited into damaged tissue, or are derived from endothelial, epithelial cells or pericytes present in the tissue that transdifferentiate into

myofibroblasts. Other potential sources of myofibroblasts have been reported including mesenchymal stem cells (MSCs), perivascular adventitial cells, and smooth muscle cells (Di Carlo and Peduto 2018).

In particular, BM derived monocytes differentiate into cells known as fibrocytes that are defined by their expression both of the pan-leukocyte marker CD45 and the fibroblast marker collagen I (Col I). Fibrocytes have been shown to be present in the target tissues of several fibrotic diseases including the lung and skin in scleroderma (SSc) and the heart of patients with cardiac disease (Quan, Cowper et al. 2004, Haudek, Xia et al. 2006, Russell, Herzog et al. 2012). Since fibrocytes originate in the bone marrow, fibrocytes or fibrocyte precursors must enter the circulation and be recruited to their target sites. The recruitment of fibrocytes to their target tissues is presumably mediated though the chemotactic action of chemokines via their interaction with cell surface chemokine receptors on circulating cells. Previous research from our lab has suggested that decreased levels of caveolin-1 in fibrocyte precursors promote the accumulation of fibrocyte derived myofibroblasts in fibrotic tissues through: 1) the increased recruitment of fibrocytes and/or their precursors (due to the upregulation of chemokine receptors) into the tissue, 2) the increased differentiation of precursor monocytes into fibrocytes in the tissue, and 3) the increased differentiation of fibrocytes into myofibroblasts that overexpress ECM proteins thereby contributing to ECM remodeling (Lee, Perry et al. 2014, Reese, Perry et al. 2014, Lee, Reese et al. 2015). Besides differentiating into myofibroblasts, fibrocytes promote fibrosis by secreting a variety of cytokines and

chemokines that activate resident fibroblasts, promote inflammation and angiogenesis, and recruit more fibrocytes and other cells to the target site.

The idea that fibrocytes serve as one of the major contributors to the population of myofibroblasts that over overexpress collagen in fibrosis is somewhat controversial (Moore-Morris, Guimarães-Camboa et al. 2014). This controversy arises from the use of different methods by different investigators. Investigators who oppose the idea that BM-derived cells contribute to fibroblast lineages may have over depended on Cre drivers for lineage specificity and the failure to stain fibrotic tissues for CD45 (Moore-Morris, Guimaraes-Camboa et al. 2014), a notoriously difficult protein to detect without proper fixation. Previously reported CD45 staining in the lungs of bleomycin-treated mice has been largely unconvincing (Inomata, Kamio et al. 2014).

Another recent study (Kleaveland, Velikoff et al. 2014) has be misinterpreted to imply that fibrocytes are not important in lung fibrosis. In fact, this study only showed that knocking out the collagen gene in BM-derived cells did not stop these cells from becoming collagen+ in fibrotic tissue by IHC. Indeed, this study states that fibrocytes normally express collagen mRNA. This study does not rule out the possibility that fibrocytes normally serve as fibroblast progenitors or that fibrocytes normally contribute to collagen expression during fibrosis. Moreover, in regard to their model, the authors state that knocking out Col I in fibrocytes may have no effect on the severity of bleomycin-induced disease because “other cell types might be compensating for loss of functional fibrocytes”.

Supporters of the importance of the monocye-fibrocyte-myofibroblast lineage (Mollmann, Nef et al. 2006, Visconti and Markwald 2006, van Amerongen, Bou-Gharios et al. 2008, Ruiz-Villalba, Simon et al. 2015) have observed a contribution of hematopoietic cells to mesenchymal cell populations in fibrotic tissue using chimeric mouse models wherein genetically-tagged (e.g. EGFP) BM cells are used to reconstitute the BM of irradiated mice. The integrated, transgenic tag is then used to trace the fate of marked cells. In summary, the EGFP genetic tag approach avoids possible problems with Cre drivers and the retention of antigenicity during fixation.

Based on this background, our goal was to refine the methods to determine whether fibrocytes (CD45+/Col I+ fibroblastic cells) truly exist, whether fibrocytes in the fibrotic lung differ from fibrocytes in control lung tissue, and whether we could determine why the fibroblasts that most people study appear to be CD45-. In addition, we examined whether a therapeutic peptide, caveolin scaffolding domain (CSD), derived from caveolin-1 affects fibrocytes. These studies have made extensive use of elegant methods including transgenic mice designed for lineage tracing, flow cytometry, and single cell sequencing.

## Materials and Methods

### Bleomycin Treatment of Mice and Harvesting of Tissue

The following procedures were approved by the MUSC Institutional Animal Care & Use Committee. Ten-week old C57BL/6 mice (Charles River Laboratories, Boston, MA) were maintained under specific pathogen-free conditions. Osmotic minipumps

(ALZET 1007D; DURECT Corporation, Cupertino, CA) containing either 100 μl saline vehicle or bleomycin (100 U/kg) designed to deliver their contents at 0.5 μ l/h for 7 days were implanted under isofluorane anesthesia under the loose skin on the back of the mice slightly caudal to the scapulae. Pumps were removed on day 8-10.

Mice were sacrificed 21-28 days after the initiation of bleomycin administration. Mice were sacrificed by isofluorane overdose, and the rib cage was opened to expose the lungs. Mice were systemically perfused via the left ventricle with PBS. The left lobe was then removed for flow cytometry, and the right lobes were collected for Western blots and histology. Lung lobes that were used for Western blots were minced and homogenized using a Tissue Tearor in 2 ml of 25 mM Tris (pH 8.0)-5 mM EDTA-5 mM EGTA plus protease inhibitors [*N*-ethylmaleimide (10 mM), benzamidine (5 mM), and phenylmethylsulfonyl fluoride (2 mM)] and phosphatase inhibitors [sodium fluoride (50 mM), sodium pyrophosphate (5 mM), and sodium orthovanadate (1 mM)]. The homogenate was centrifuged for 3 min at 16,000 *g*. Finally, the supernatant was boiled for 3 min in SDS-PAGE sample buffer for use in Western blotting experiments using the indicated primary antibodies and appropriate secondary antibodies. If the right lobe was used for histology, the left lobe was tied off and cut off. The remaining right lobes were perfused with buffered zinc formalin fixative (Z-Fix; Anatech, Battle Creek, MI). Fixed lung tissue was then removed and embedded in paraffin. Sections (4 μm) were stained with hematoxylin and eosin (H&E) or Masson's trichrome or immunohistochemically.

## Cell Culture

All cell culture experiments were performed using DMEM with 4.5 g/L glucose, L-glutamine, and sodium pyruvate containing 10% FBS with antibiotic/antimycotic solutions. The cells were maintained at 37°C and 5% CO2.

## Adhesion Assay

For the adhesion assay, cells were lifted using accutase for 10 minutes at 37°C. The enzyme was inactivated with 10% DMEM/FBS, and the cells were spun for 5 seconds in the centrifuge to remove clumps. The supernatant was then transferred to a new tube, and washed 2 times with DMEM/20 mM HEPES (pH 7.3), before being resuspended to 300,000 cells/mL to be plated at 100 µl per well. Prior to plating the cells, a non-tissue culture plastic 96-well plate was prepared by coating the wells with 100 µl of 0.1 M sodium bicarbonate in PBS containing either 0, 1, 3, 10, or 30 µg/mL of fibronectin. The wells were then blocked for 1 hour with 200 µl of 10 mg/mL BSA in 0.1 M sodium bicarbonate. Cells were then added to the plate and incubated for 1 hour at 37°C and 5% CO2. After 1 hour, the plates were washed by submersion in warm PBS two times with gentle shaking. The PBS was poured off and the cells were fixed for 5 minutes with 10% EtOH, and washed with PBS. The wells were then observed and photographed on a fluorescent microscope, and images were quantified using Fiji – ImageJ.

**Bronchoalveolar Lavage (BAL) Collection**

Mice were sacrificed by isofluorane overdose, and the trachea was exposed. A small incision was made in the top half of the trachea to allow the insertion of a blunted 20-gauge cannula. The cannula was then secured in place by tying a knot around the inserted cannula in the trachea using suture thread. A 1 mL TB syringe containing approximately 900ul of HBSS with 100 uM EDTA and antibiotic/antimycotic solution was connected to the cannula, and used slowly to flush the lungs and recover the solution. This process was repeated 4 times. After collection, cells were collected by centrifugation (1200 rpm, 10 min, 4°C, Beckman GS-6R centrifuge) and the cell pellets resuspended in 1 ml ACK red blood cell lysing buffer (LONZA #10-548E) for 5 min to remove red blood cells. The cells were then collected by centrifugation, washed, and resuspended in the collection buffer.

**EGFP Bone Marrow Transplantation**

Ten to 14-week-old male C57BL6/Ly5.1 mice were prepared for bone marrow transplantation using a single dose (9.0 Gy) of total body irradiation. Ten to 12-week-old female EGFP/Ly5.2 mice were used as donors (Visconti et al., 2006). These mice express EGFP under the control of a chicken beta-actin promoter and cytomegalovirus enhancer, and have EGFP fluorescence in all cells, with the exception of erythrocytes and hair. Briefly, donor mice were humanely sacrificed by $CO_2$ inhalation. Bone marrow cells were flushed from femurs and tibiae and washed in $Ca^{++}$- and $Mg^{++}$-free phosphate-buffered saline containing 0.1% BSA. A monodisperse suspension was prepared by gentle trituration and filtering through a 40-μ m filter. Mononuclear cells were isolated by

density gradient centrifugation using Lympholyte-M (Cedarlane Labs, Burlingame, NC). $2.0\times10^5$ of these EGFP+ donor bone marrow cells were transplanted into the irradiated recipients by tail vein injection. As previously described (Visconti et al., 2006), peripheral blood chimerism was assayed at 30 days post-transplantation and multi-lineage hematopoietic reconstitution was assayed at 60 days. Mice exhibiting high levels of reconstitution were used in subsequent studies.

**Collagen-EGFP Mice**

These mice were generously donated by Drs. Carole Wilson and Lynn Schnapp (while they were at the Medical University of South Carolina, now at University of Wisconsin-Madison. Briefly, these transgenic C57BL/6 mice express EGFP under the control of the *Col1a1* promoter, allowing for the monitoring of type I collagen producing cells based on EGFP fluorescence without requiring the use of antibodies (Yata, Scanga et al. 2003).

**Vav1-Cre;mTmG Mice**

The Vav1-Cre;mTmG mice for this study were generated from two types of commercially available mice from Jackson Labs, Vav1-Cre mice (B6.Cg-Tg(Vav1-icre)A2Kio/J, stock #008610) and two-color fluorescent Cre reporter mice (B6.129(Cg)-Gt(ROSA)26Sor$^{tm4(ACTB-tdTomato,-EGFP/Luo}$/J, stock #007676), abbreviated ROSA-mTmG. Vav1-Cre mice were obtained as hemizygotes (Vav1-Cre/+) whereas the ROSA-mTmG mice were available as homozygotes (mTmG/mTmG). Both of these mice strains are made on a C57BL/6 background. For use in the experiments, mice with the Vav1-

Cre/+;mTmG/+ and Vav1-Cre/+;mTmG/mTmG were used. Under this genotype, hematopoietic or BM derived cells (Vav1) will express the membrane targeted green fluorescent protein (mG) via Cre mediated excision, while all other cells will express membrane targeted tandem dimer Tomato (mT) (Figure 1) (Muzumdar, Tasic et al. 2007).

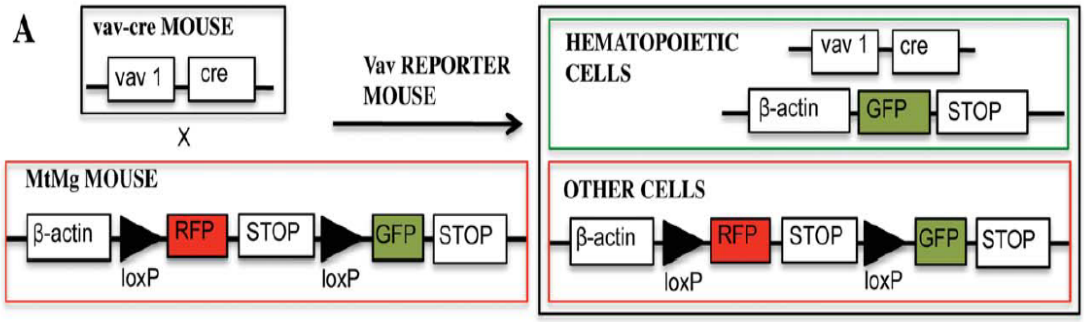


**Figure 1. Vav1-Cre+/mTmG Diagram.** Schematic representation showing Cre mediated excision of the GFP protein in Vav1 expressing cells, while all other cells will express the RFP, tdTomato.

**CSD Treatment of Mice**

Vav1-Cre+/mTmG mice were treated with either saline or bleomycin as described above. Seven days after bleomycin administration, mice that received bleomycin began receiving daily intraperitoneal (IP) injections of either vehicle or water soluble CSD (WCSD) (concentration). Injection sites were alternated daily to minimize stress and irritation to the abdomen of the mice. Mice were sacrificed 21 days after the administration of bleomycin, and BAL, lung, and skin specimens were collected as described above.

**Flow Cytometry**

Lung tissue from mice was washed in cold DMEM and minced into small pieces using fine surgical scissors. The tissue from each mouse was resuspended in 5 ml of collagenase (1 mg/ml, Roche #10103578001) and shaken at low speed for 45 min at 37°C. Digestion was stopped by addition of 10 ml of DMEM/10% FBS. The sample was passed through a 40 μm cell strainer to prepare a monodisperse cell suspension. Cells were collected by centrifugation (1200 rpm, 10 min, 4°C, Beckman GS-6R centrifuge) and the cell pellets resuspended in 1 ml ACK lysing buffer (LONZA #10-548E) for 5 min to remove red blood cells. Lung cells were then collected by centrifugation, washed with PBS, collected, and fixed and permeabilized for 20 min at 4°C in 1 ml Cytofix/Cytoperm (BD #554722). Finally, cells were washed in FACS buffer containing Fetal Bovine Serum (FBS) and saponin (BD Perm/Wash Buffer 554723) and resuspended in an appropriate volume of FACS buffer prior to staining.

All incubations with antibody were done for 30 min at 4°C on a rocker at low speed, all washes were done with FACS buffer, and all resuspensions were with FACS buffer. Following washing, the immunolabeled cell suspension was analyzed by FACS using a MoFlo Astrios (Beckman Coulter) or a Guava easyCyte 8HT (Millipore). At least 5,000 events were recorded per sample.

**Single Cell RNA Sequencing**

Experimental procedures followed established techniques using the Chromium Single Cell 3’ Library v3 Kit (10x Genomics;

https://assets.ctfassets.net/an68im79xiti/40xc58fJNcCWipI1YIdXoS/a87092c1c1faa0f316c552a97229a268/CG000185_ChromiumSingleCell3_v3_FeatureBarcoding_CellSurfaceProtein_UG_Rev_D.pdf). Briefly, cultured cells in single-cell suspension were labeled with TotalSeq™-B anti-mouse Hashtag antibodies (Biolegend) and pooled in equal proportions prior to loading onto a 10X Genomics Next GEM Chip B and emulsified with Single Cell 3' GEM beads using a Chromium™ Controller (10x Genomics). From the barcoded cDNAs, gene expression (GEX) libraries were constructed using Chromium™ Single Cell 3′ GEM Library Kit and hashtag oligo (HTO) libraries were constructed using Chromium™ Single Cell 3′ Feature Barcode Library Kit (both from 10X Genomics) at the Translational Science Laboratory (Medical University of South Carolina). RNA sequencing was performed on each sample (approximately 50,000 reads/cell for GEX libraries and 5000 reads/cell for HTO libraries) using a NovaSeq S4 flow cell (Illumina) at the VANTAGE facility (Vanderbilt University Medical Center).

For this study, lung cells were isolated from saline (n=3) and bleomycin (n=3) treated Vav1-Cre+/mTmG mice and cultured in 10% DMEM and grown until near confluence. Cells were lifted with accutase, washed, counted, and 50,000 cells from each sample were incubated with mouse Tru-Stain FcX (Biolegend) for 10 minutes on ice (in PBS + 1% BSA), then incubated with 1 ug anti-mouse Hashtag antibody for 30 minutes on ice (in PBS +1% BSA) at a final concentration of 500 cells/μL. Labeled cells were then washed three times with 1.5 mL of PBS + 1% BSA, resuspended in 50 μL of PBS + 0.04% BSA, and counted (Cellometer K2, Nexcelom Biosciences) before pooling. RNA

sequencing was the performed on each of the 2 pools (bleomycin and saline) containing approximately 17,400 cells each.

**Statistical Analyses**

All numerical data are expressed as average ± standard deviation and were analyzed using the Student's *t*-test to evaluate statistical significance using GraphPad Prism 7. In all figures, statistical significance is expressed as $*p < 0.05$, $**p < 0.01$, and $***p < 0.001$.

**Results**

**CD45+/Col I+ Cells are Increased in the Bleomycin Lung**

To assess whether CD45+/Col I+ cells were elevated in fibrotic lungs, mice were treated with either saline (n=11) or bleomycin (n=17) using the Pump Model (Lee, Reese et al. 2014), and sacrificed at day 28. Total lung cells were isolated and double labeled using antibodies for CD45 and an antibody against collagen Ia1 C-terminal propeptide (Col I), and examined by flow cytometry. To establish the gating strategy for both CD45 and Col I, a fluorescence minus one (fmo) approach was used in which total lung cells were incubated with CD45 only, or pro-collagen only antibodies (data not shown). For this analysis using the MoFlo Astrios flow cytometer, the data from the 2D scatter plots was split into four regions: Region I ($CD45^{high}$/Col I+), Region II (CD45+/Col I+), Region III (CD45+/Col I-), and Region IV (CD45-). Using this strategy, bleomycin treated mice showed a significant increase in both Regions I ($p < 0.001$) and II ($p < 0.01$)

(Figure 2). Interestingly. the saline treated mice contained almost no cells in Region I (CD45high/Col I+).

To further examine the accumulation of CD45+/Col I+ cells in the lung, a time course experiment was performed using the same parameters discussed above looking at Days 3, 10, and 28 post-pump implantations (Figure 2). Saline treated mice (n=3) showed low numbers of Region I (CD45high/Col I+) cells throughout the whole-time course experiment, while bleomycin treated mice (n=3) showed a drastic increase in the number of cells in Region I (CD45high/Col I+) that was significantly different than saline treated mice at Day 28 ($p < 0.001$). In Region I (CD45+/Col I+), there was a significant increase ($p < 0.01$) in the percentage of cells in both saline and bleomycin mice observed at Day 3 that was not seen at Days 10 and 28. Additionally, naïve mice were examined, and there were no more than 4% of positive cells in Region I (CD45+/Col I+) (data not shown). This increase in Region I (CD45+/Col I+) cells at Day 3, observed in both saline and bleomycin, dropped after 10 days, and indicates the implantation of the pump as the cause for this increase, rather than the contents of the pump. By Day 28, the percentage of positive cells in the saline mice remained unchanged in Region I (CD45high/Col I+), and stayed at the same percentage observed at Day 10 for Region I (CD45+/Col I+). For the bleomycin treated mice there was a statistically significant ($p < 0.05$) increase in the percentage of positive cells between the 10-day level and 28-day levels in Region I (CD45high/Col I+) (not marked), that was also significantly different from the percentages in saline mice. For Region I (CD45+/Col I+), the percentage of positive cells followed the same pattern as the saline mice and stayed relatively unchanged from Day

10 to 28. These experiments indicate that there is always a population of CD45+/Col I+ cells in the lungs, and there is a significant increase in both CD45$^{high}$/Col I+ and CD45+/Col I+ cells in the bleomycin treated mouse lung that accumulates over time.

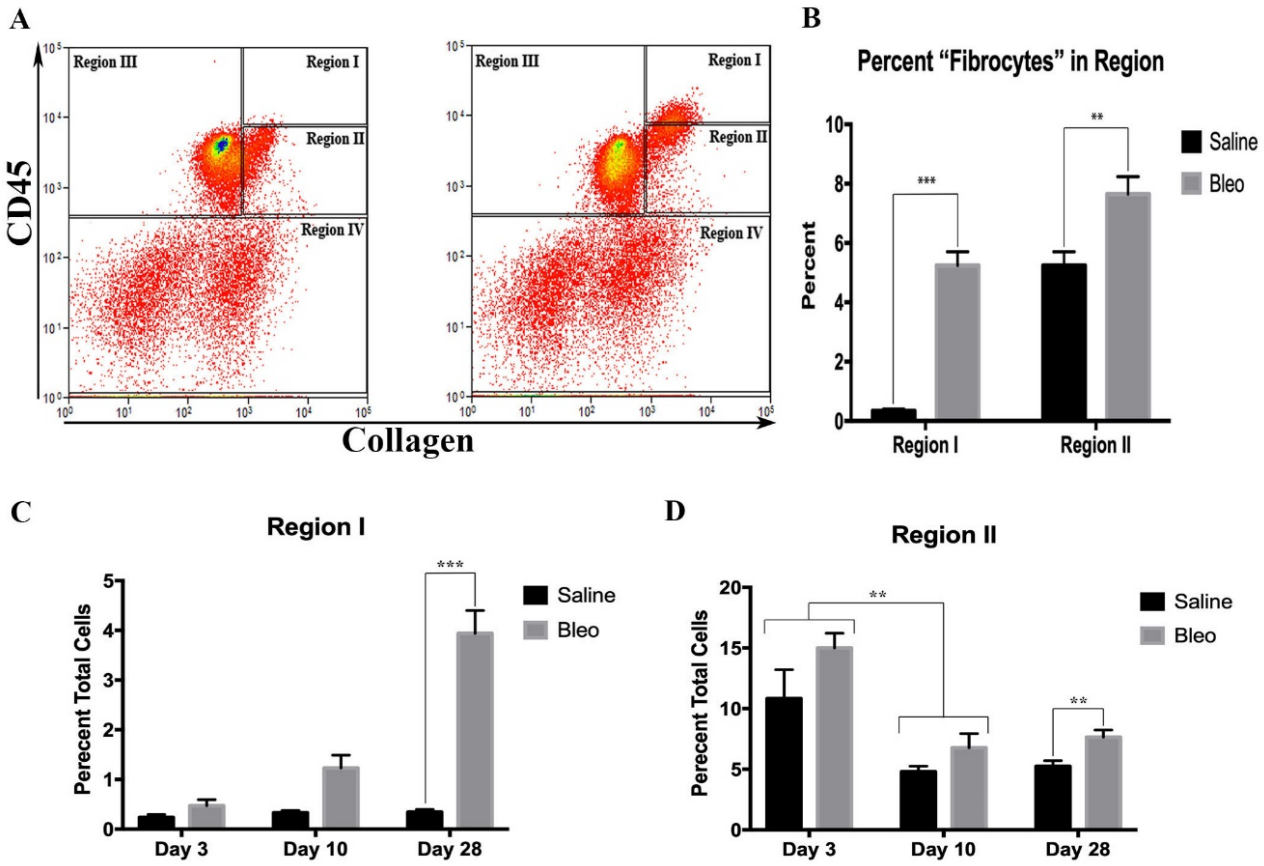


**Figure 2. Quantification of Fibrocytes in the Lung Over Time (A)** Total lung cells from both saline and bleomycin-treated mice were labeled with antibodies for CD45 and Col I. Two-dimensional scatter plots are represented with CD45 on the y-axis and Col I on the x-axis. The 2D plots were split into Regions I-IV and used throughout this experiment. **(B)** The percent of total lung cells in Region I (CD45$^{high}$/Col I+) and II (CD45+/Col I+) are shown in terms of average ± SD of the 11 saline and 17 bleomycin-treated mice sacrificed 28 days after the initiation of treatment. The percent of total lung cells in Region I (CD45high/Col I+) **(C)** or II **(D)** 3, 10, or 28 days after saline or bleomycin treatment is shown as the average ± SD for the following number of mice in each category: 3-day saline, n=3; 3-day bleomycin, n=3; 10-day saline, n=3; 10-day bleomycin, n=3; 28-day saline, n=11; 28-day bleomycin, n=17. Since there were no differences observed in the percent of cells in Region I (CD45+/Col I+) between saline

and bleomycin lung at day 3 and day 10, saline and bleomycin data were pooled before determining the statistical significance in the decrease in percent of cells in Region I (CD45+/Col I+) between day 3 and day 20. ***p < 0.01, ***p <0.001.*

**HSP47 Levels are Increased in the Bleomycin Lung**

The collagen chaperone, HSP47, has been found to be upregulated in the fibrotic tissues of the heart, liver, and lung in humans as well as in experimental models of fibrosis in mice. HSP47 plays an important role in the processing of procollagen, and can serve as a surrogate marker for collagen expression (Lee, Reese et al. 2014, Otsuka, Shiratori et al. 2017, Khalil, Kanisicak et al. 2019, Miyamura, Sakamoto et al. 2020). As stated above, mice were sacrificed 28 days after the administration of either bleomycin or saline, and total lung cells were isolated by collagenase digestion. The lung cells were then stained with antibodies for CD45, Col I, and HSP47 (Figure 3). Regions I and II examined using the gating strategy from (Figure 2) showed higher levels of staining for HSP47 in the mice that had received bleomycin (Figure 3). There was a statistically significant difference in HSP47 expression in both Regions I and II, where CD45+/Col I+ cells are located. Region I (CD45+/Col I-), containing CD45+/Col I- cells showed very low expression of HSP47. Cells from both saline and bleomycin treated mice showed expression of HSP47 in Region IV, where CD45- cells are located. Of note, in cells from the bleomycin treated mice, there was a larger population of cells in Region 4 (CD45- cells) with very high mean fluorescent intensity (MFI), than was present in the cells isolated from the saline mice (Figure 3).

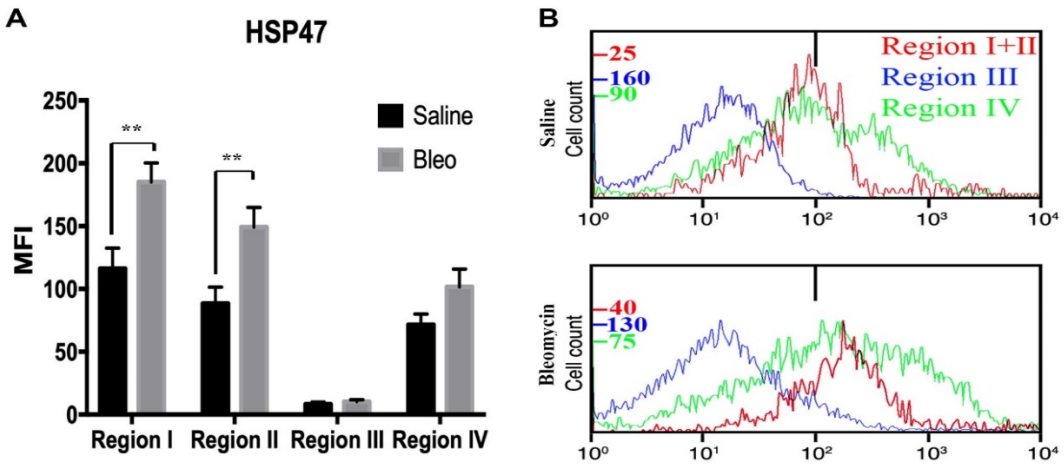


**Figure 3. Collagen Chaperone HSP47 in Regions I-IV. (A)** Total lung cells were labeled with antibodies for CD45, Col I, and HSP47 28 days after the treatment with saline or bleomycin. Regions I-IV are shown in terms of average ± SD of the MFI of each of 11 saline and 17 bleomycin treated mice. **(B)** Cells from Region I+II (CD45+/Col I+), Region III (CD45+/Col I-), and Region IV (CD45-) were selected and the MFI of HSP47 in these cells was plotted. The bar at 1 x $10^2$ represents that maximum MFI for unstained cells. Note the increased MFI values observed in Regions I+II and Region I (CD45-) for bleomycin treated mice. $**p < 0.01$

**Circulating Fibrocytes**

To determie if fibrocytes could be found in the blood, blood was collected at 3, 10, and 28 days after the administration of bleomycin or saline. Mice were sacrificed and peripheral blood mononuclear cells (PBMCs) were isolated from blood collected by cardiac puncture (Figure 4). Using the same gating strategy from above (Figure 3), virtually no cells were detected in Region I (CD45high/Col I+) at any time point studied, and very small numbers of cells were found in Region I (CD45+/Col I+). For both saline and bleomycin-treated mice, there was a large difference in the number of cells found in Region I (CD45+/Col I+) at day 3 versus the other two time points. However, there were no real differences observed between saline and bleomycin at any of the individual time points that were studied. This increase seen in the number of cells in Region I

(CD45high/Col I+) and II at day 3 was also observed in the total lung cells (Figure 2). These observations strongly suggest that after the implantation of the pump, cells from the bone marrow are recruited into circulation in response to the inflammation caused by the surgery. This is further reinforced by the observation that by day 10 and 28, it is very difficult to detect cells in Regions I and II. These observations suggest that CD45+/Col I+ cells found in both Regions I and II are either recruited from the circulation at an early time point, or that these cells do not fully differentiate into CD45+/Col I+ cells found in Regions I and II until after they enter the lung.

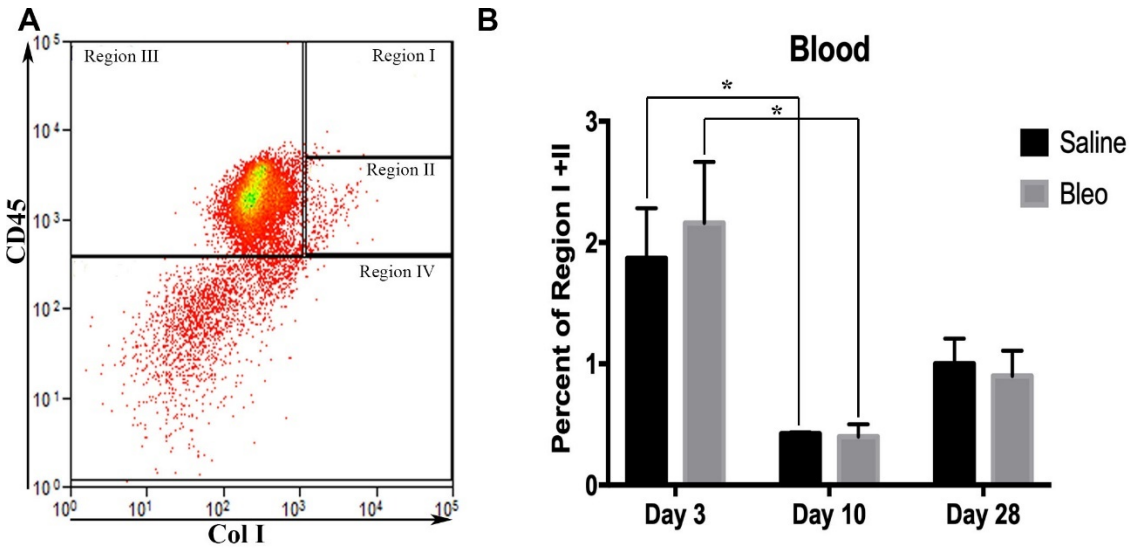


**Figure 4. Circulating Fibrocytes**. **(A)** PBMCs were collected from both saline and bleomycin-treated mice 28 days after pump implantation, and stained with antibodies for CD45 and Col I. A 2D-plot from a bleomycin-treated mouse is shown with CD45 on the y-axis and Col I on the x-axis (saline not shown). Note that there are almost no cells present in Region I (CD45high/Col I+) and few cells in Region I (CD45+/Col I+), this distribution of cells was observed in both saline and bleomycin-treated mice. **(B)** Percent of PBMCs found in Region I+II expressed as the average ± SD for 3 saline and 3 bleomycin-treated mice at days 3, 10, and 28. Note the significant decrease in percent of Region I+II from day 3 to 10 observed in both saline and bleomycin PBMCs. *$p < 0.05$

**EGFP-BM Transplanted Mice Confirm that CD45+/Col I+ Cells are BM Derived**

To confirm that the cells found in Regions I and II in the above experiments

(Figure 2) were BM derived, a mouse model in which mice were first irradiated, and then transplanted with the BM from an EGFP-mouse was used (Figure 5). Similar to the experiments outlined above, saline (n=3) and bleomycin-treated (n=3) mice reconstituted with BM from EGFP-mice were sacrificed after 28 days, and total lung cells were isolated. The cells were then labeled with antibodies for CD45 and Col I and analyzed by flow cytometry. A similar 2D profile was observed, and the cells were grouped into three Regions: Region I containing all CD45+/Col I+ cells (Regions I+II from Figure), Region II containing CD45+/Col I- cells, and Region 3 containing all CD45- cells (Figure 5). Cells found both in Regions I and II (Regions I-III from below) were 100% EGFP+, while cells found in Region III contained mostly EGFP- cells and only about 10% EGFP+. These observations support the idea that BM derived cells can contain collagen, and that this pattern of EGFP expression mirrors the expression of CD45, a hematopoietic cell marker expressed on all BM derived cells.

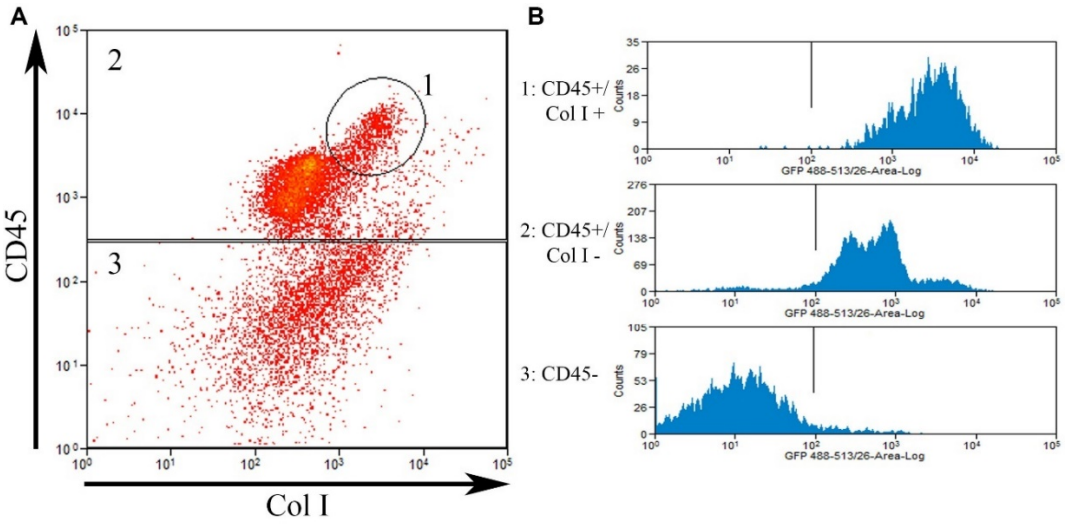


**Figure 5**. **CD45+/Col I+ Cells are BM derived. (A)** To confirm that the cells in Regions I and II (CD45+) where BM derived, total lung cells were isolated from saline (n=3) and

bleomycin (n=3) mice reconstituted with bone marrow expressing EGFP, and stained with CD45 and Col I. Bleoymcin-treated lung cells are shown. **(B)** Cells in the defined regions 1-3 are shown in 1D plots of MFI for GFP. Nearly 100% of cells in Regions 1-2 were positive for GFP, while cells in Region 3 were only 10% positive for GFP.

Additionally, lung tissue was collected for IHC analysis from bleomycin and saline-treated mice 28 days after pump implantation, and was stained with antibodies for Col I and EGFP (Figure 6). Both saline and bleomycin treated mice had EGFP positive cells in their lungs, but the bleomycin mouse lung had considerably more EGFP positive cells and this staining overlapped with the increased collagen staining seen in the bleomycin lung. This observation supports the idea that many EGFP-positive cells from transplanted BM end up in the fibrotic lung as collagen positive cells.

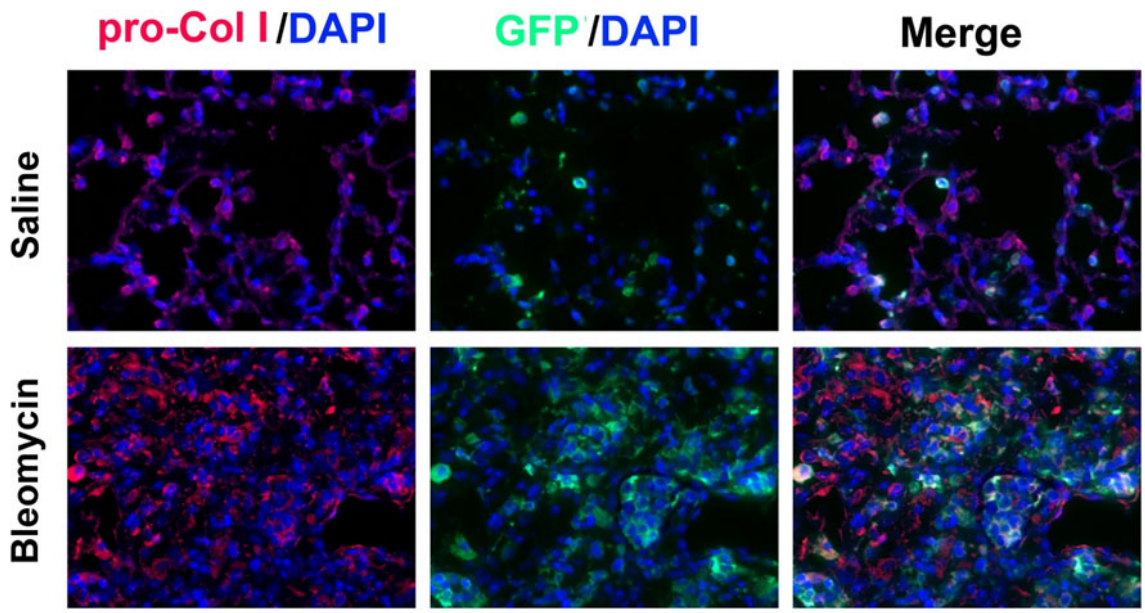


**Figure 6. BM-GFP+ Cells are Col I+ in the Lung Tissue.** Lung tissue was stained with antibodies for Col I (red) and GFP (green) for immunofluorescent analysis. Staining revealed an increase in Col I expression in the bleomycin-treated mouse, and many of these cells also expressed GFP indicating their hematopoietic origin.

**Collagen-EGFP Mice**

To further characterize CD45+/Col I+ cells by flow cytometry, mice that express EGFP under the collagen promoter were used to allow for further examination of cells that were CD45+/Col_EGFP+ without relying on the use of an anti-collagen antibody. Ten to 12-week old collagen-EGFP mice were treated with bleomycin (n=3) or saline (n=3) using the pump model and sacrificed after 21 days. Total lung cells from these mice were double labeled with antibodies for CD45, and various monocyte/macrophage markers, and examined by flow cytometry (Figure 7). A significant increase in the number of CD45+/Col_EGFP+ cells was observed in the bleomycin-treated mouse compared to the saline mouse. This result was similar to the data we obtained using lung cells from both C57BL/6 mice (Figure 2), and EGFP-BM transplanted mice (Figure 6).

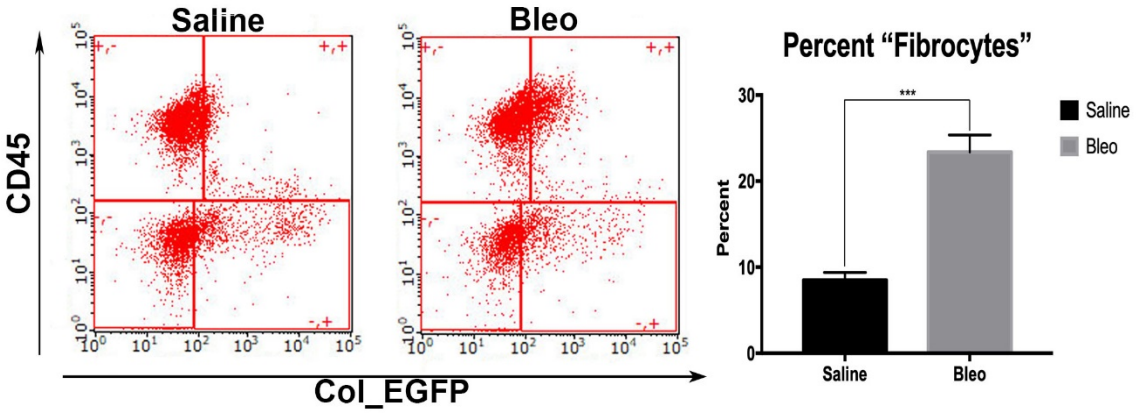


**Figure 7. CD45+ Cells from Bleomycin-Treated Mice Express Col I at Enhanced Levels. (A)** Total lung cells were isolated from Col_EGFP mice 28 days after bleomycin or saline-treatment by osmotic mini pump, and labeled with CD45 antibody. Scatter plots are presented with CD45 on the y-axis and Col_EGFP on the x-axis. **(B)** Fibrocytes (CD45+/Col_EGFP+) are shown in terms percent positive ± SD showing a statistically significant increase in the number of CD45+/Col_EGFP+ cells in the bleomycin lung. ****p < 0.001.*

Additionally, the cell populations that were CD45+/Col_EGFP- and CD45+/Col_EGFP+ were examined for their expression of the monocyte/macrophage markers CD16, CD68, and CD206. While similar low expression levels of CD16, CD68, and CD206 was observed on CD45+/Col_EGFP- in cells from both saline and bleomycin that were little more than unstained levels, they were present at much higher levels on CD45+/Col_EGFP+ cells from the bleomycin-treated lung compared to the saline-treated lung (Figure 8). These data further support the idea that CD45+/Col I+ cells increase in the fibrotic lung and that they not only express the fibrosis markers Col I and HSP47, they also express higher levels of monocyte/macrophage markers than CD45+/Col I- cells. Moreover, the levels of these markers are higher in CD45+/Col I+ cells from bleo than saline.

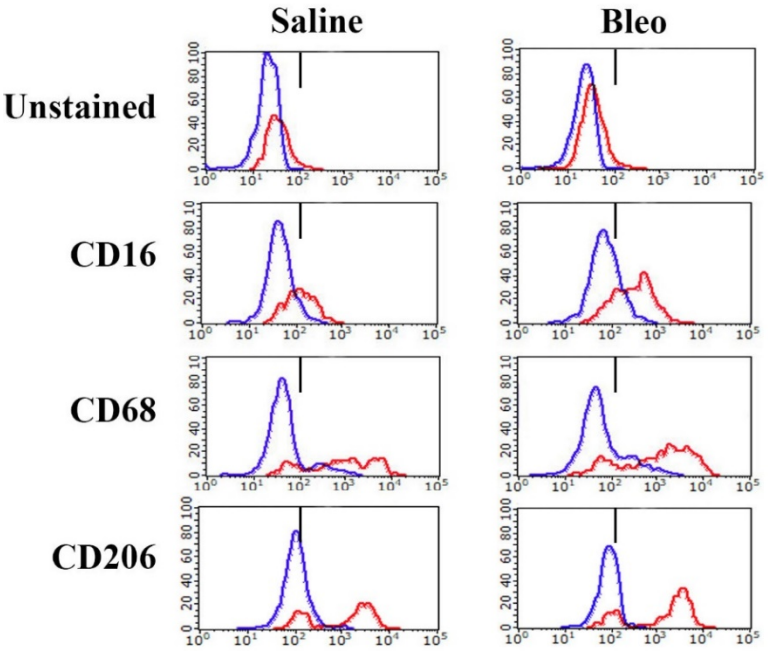


**Figure 8. CD45+/Col_EGFP+ Cells Contain High Levels of Monocyte/Macrophage Markers.** To examine the expression level of monocyte/macrophage markers on

CD45+/Col_EGFP+ cells, 1D plots were generated gated on CD45+/Col_EGFP- (blue) and CD45+/Col_EGFP (red) based on the regions defined in Figure 7. Similar expression levels of CD16, CD68, and CD206 were observed on CD45+/Col_EGFP- cells from both saline and bleomycin-treated mice, while expression of these markers was much higher in CD45+/Col_EGFP+ cells from bleomycin-treated mice than from saline. Interestingly, expression levels for all markers examined was higher in CD45+/Col_EGP+ than CD45+/Col_EGFP- cells.

**Vav1-Cre;mTmG Mice Show the Hematopoietic Contribution to Myofibroblasts**

To provide further evidence that hematopoietic cells can contribute to the population of myofibroblasts found in the lung, transgenic mice containing hematopoietic or BM derived cells (Vav1+) that express membrane targeted GFP via Cre mediated excision were used. All other cells in this model will express membrane targeted tdTomato. These mice were treated with either bleomycin (n=4) or saline (n=4) using the pump model (Lee, Reese et al. 2014), and sacrificed at 21 days past pump implantation. Both BAL and total lung cells were isolated from the mice, and double labeled with antibodies for CD45 and Col I as well as various other monocyte/macrophage and fibrosis related antibodies. The cells were then analyzed by flow cytometry (Figure 9 and 10). To establish a gating strategy for the analysis, both BAL and lung cells were run through the flow cytometer without any primary antibody and are shown in Figures 9 and 10.

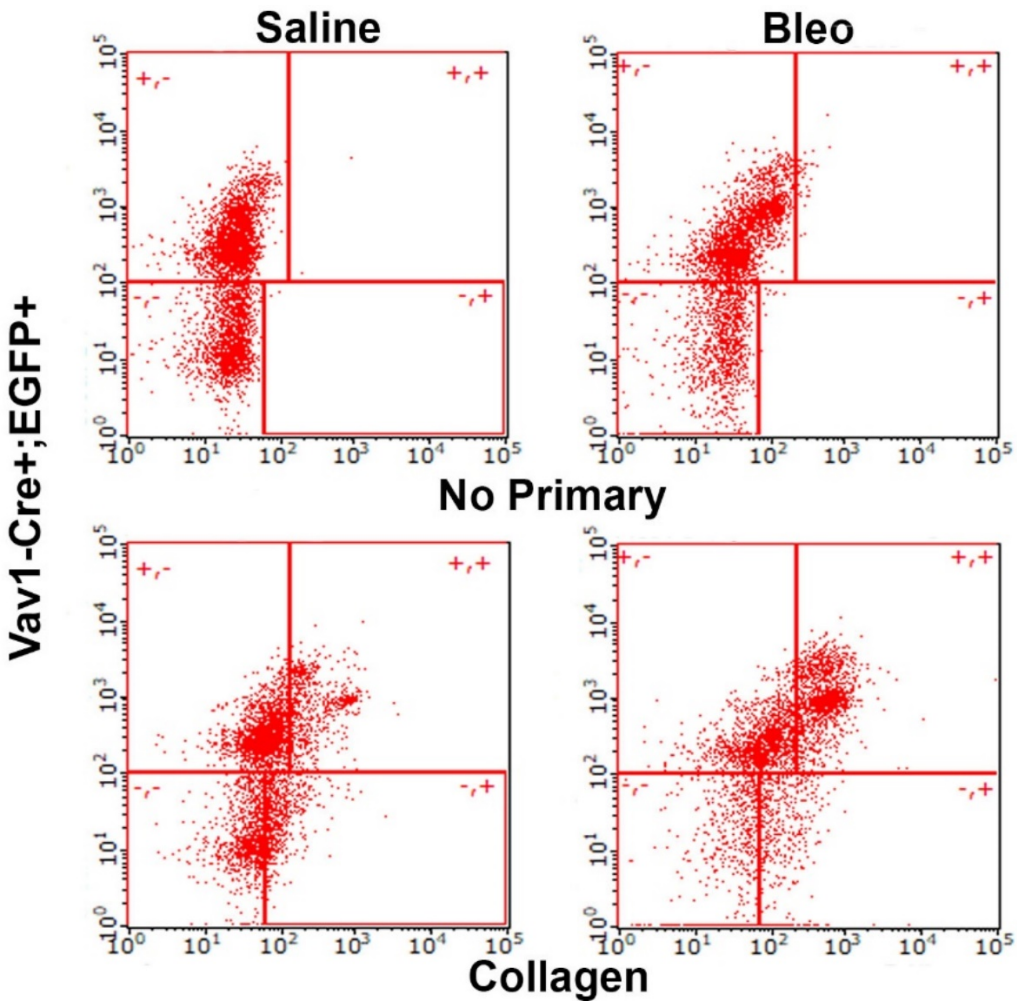


**Figure 9. Vav1-Cre+;EGFP+/Col I+ Cells are Increased in the Bleomycin Lung.** Total lung cells were isolated from saline (n=4) and bleomycin-treated (n=4) mice 21 days after pump implantation, and labeled with Col I antibody. The gating strategy was established by using unstained cells for both saline and bleomycin mice seen in the top two panels. A significant increase in the number of Vav1+/Col I+ cells was seen in the bleomycin mouse lung, with no apparent change in Vav1-/Col I+ cells as seen in previously reported experiments using other models. These experiments offer further support that hematopoietic cells express collagen in increased numbers in fibrosis.

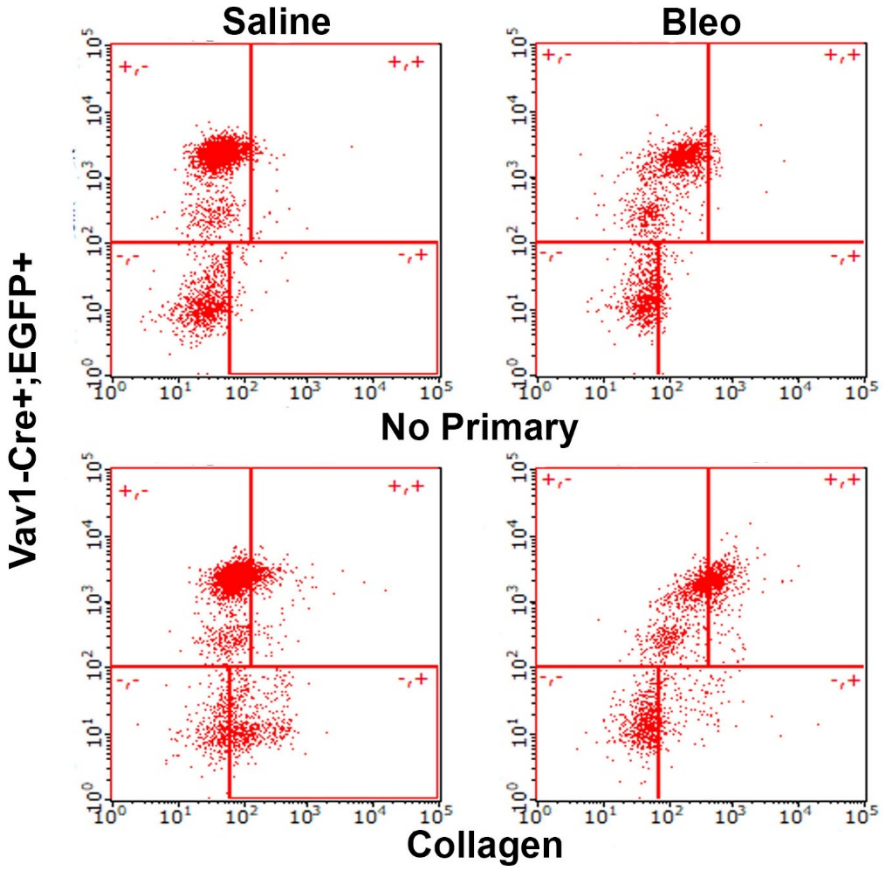


**Figure 10. Vav1-Cre+;EGFP+/Col I+ Cells are Increased in the BAL from Bleomycin-Treated Mice. C**ells were isolated from the BAL of saline (n=4) and bleomycin-treated (n=4) mice 21 days after pump implantation, and labeled with Col I antibody. The gating strategy was established by using unstained cells for both saline and bleomycin mice seen in the top two panels. A significant increase in the number of Vav1-Cre+;EGFP++/Col I+ cells was seen in the BAL cells from the bleomycin mouse lung compared to saline BAL. This observation was similar to the results obtained when looking at total lung cells.

Examination of the data from the bleomycin and saline-treated mice showed a significant increase in the number of Vav1-Cre+;EGFP++/Col I+ cells from both the bleomycin BAL and lung as compared to the saline BAL and lung. This same observation was observed when CD45 replaced Vav1-Cre+;EGFP+ on the Y-axis (Figure 11). These observations provide even further proof that hematopoietic cells can express collagen and contribute to the myofibroblast population in fibrotic tissues. Additionally,

the BAL and lung cells were further analyzed for their expression of monocyte/macrophage markers, as well as selected fibrosis markers by gating on Vav1-Cre+;EGFP++ (similar results were obtained by gating on CD45+ and are not shown). Histograms showing representative MFI values for these cells are shown in Figure 12. The analysis of Vav1-Cre+;EGFP+ cells from the total lung revealed a significant increase in collagen. Additionally, there was a major increase in the number of cells expressing the monocyte and macrophage markers CD11b, CD16, and CD68 in the bleomycin-treated mice compared to the saline-treated mice (similar to the results in Figures 7 and 8). Quantification of this analysis is shown in Figure 13.

In the analysis of the BAL cells, it was found that the number of cells expressing the monocyte and macrophage markers, CD11b and CD16, was significantly increased in bleomycin-treated mice compared to saline-treated mice. Similar to the Vav1-Cre+;EGFP+ cells from the total lung, the number of cells expressing collagen was significantly increased in the BAL of bleomycin-treated mouse.

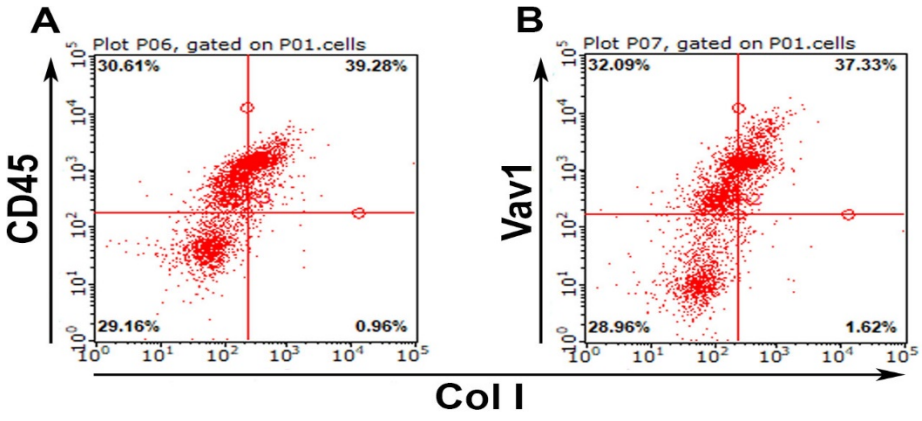


**Figure 11. CD45 and Vav1-Cre+;EGFP+ Show Similar Profiles When Labeled with Col I.** To examine if CD45 and Vav1-Cre+;EGFP+ are labeling the same cell populations, total lung cells isolated from bleomycin-treated mice were labeled with

CD45 and Col I antibodies, and 2D Scatter plots were made. **(A)** Scatter plot showing CD45 on the y-axis and Col I on the x-axis. **(B)** Scatter plot showing Vav1-Cre+;EGFP+ on the y-axis and Col I on the x-axis. These scatter plots show that both CD45 and Vav1-Cre+;EGFP+ give similar results when labeling fibrocytes. Similar results were also obtained with saline-treated samples.

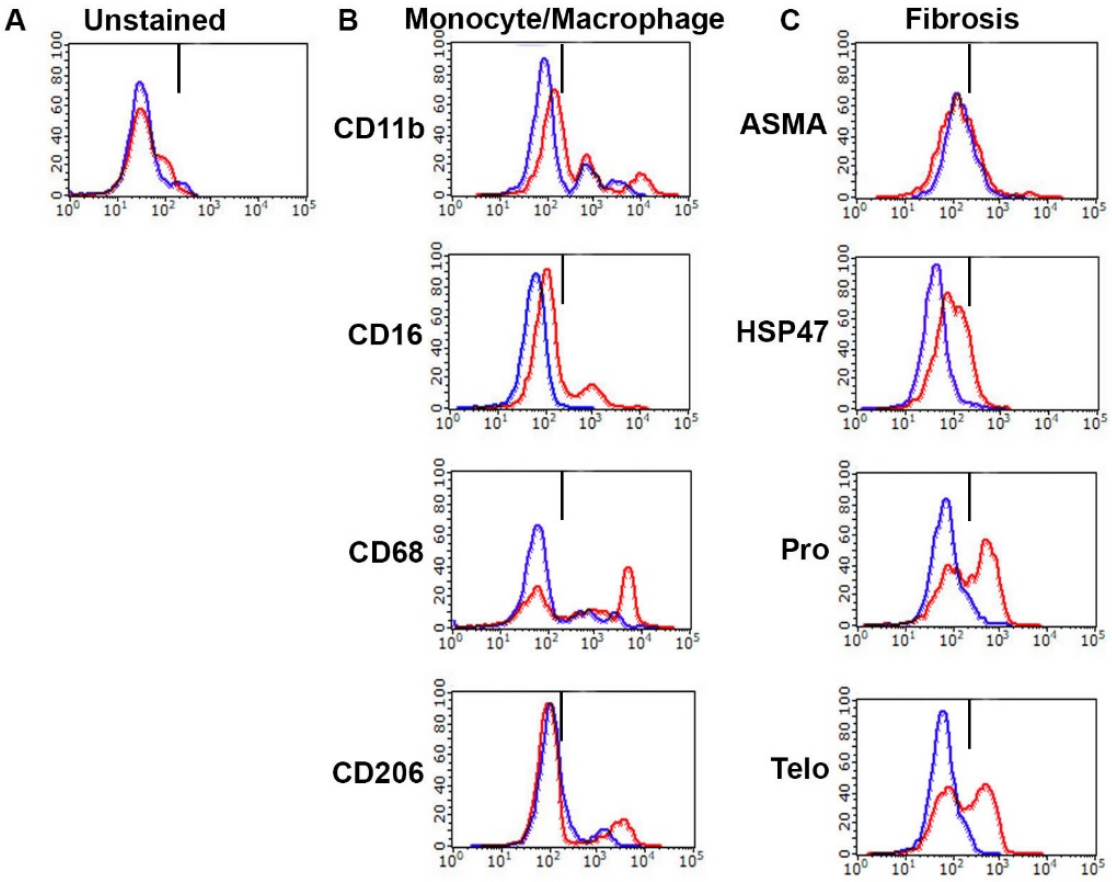


**Figure 12. 1D Plots of Vav1+ Cells in Total Lung Cells.** To visualize the differences in monocyte/macrophage and fibrosis markers between saline (blue) and bleomycin-treated (red) mice, 1D plots of Vav1+ cells are shown for **(A)** unstained, **(B)** monocyte/macrophage markers, and **(C)** fibrosis related markers. Note the higher MFI values in Vav1+ cells from bleomycin-treated (red) mice compared to saline (blue) particularly for CD11b, CD16, CD68, CD206, and both collagens.

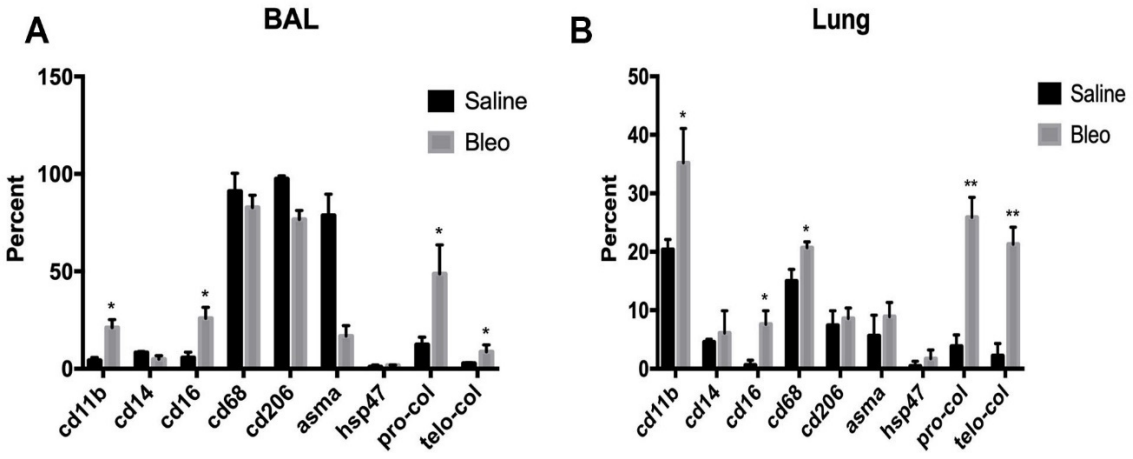


**Figure 13. Characterization of Vav1+ cells from BAL and Total Lung. (A)** Cells isolated from the lungs of saline (n=4) and bleomycin-treated (n=4) mice 21 days post pump implantation were gated on Vav1-Cre+;EGFP+ expression and analyzed for monocyte/macrophage markers and various fibrosis markers. CD11b and CD16 cells were increased in the BAL of bleomycin-treated mice when compared to saline-treated mice. Cells expressing both pro and telo-collagen were also significantly increased in the bleomycin BAL. **(B)** Total lung cells from the same experiment were also analyzed for the same markers 21 days post pump implantation, revealing significant increase in the number of CD11b, CD16, and CD68 cells in the lung tissue. Both pro and telo-collagen were also significantly increased in the total lung tissue of bleomycin-treated mice. *$p < 0.05$, **$p < 0.01$*

**Growth of Fibroblast from Vav1-Cre;mTmG Mice**

As many researchers define fibroblasts as CD45- cells, it was important to determine the fate of CD45+ (Vav1-Cre+;EGFP+) cells in standard fibroblast cultures. Therefore, an experiment was performed where total lung cells were isolated from Vav1-Cre;mTmG mice (n=3) and cultured under established fibroblast growth conditions. Briefly, cells from total lung tissue were dissociated using collagenase, and were seeded using DMEM+10% FBS in either T-25 flasks at a standard seeding density of $0.7 \times 10^6$ or in 6 wells plates at a standard seeding density of $0.3 \times 10^6$, allowed to attach overnight, and then non-adherent cells were washed off the next day. Cells were cultured and

examined under a fluorescent microscope by assessing 3 randomly selected high-power fields (HPF) from the plates at each time point. Passaging of cells was done with Trypsin/EDTA. Cells that had not undergone any passages (P0), contained significantly higher numbers of Vav1-Cre+;EGFP+ cells, than those that had been passaged once (P1) (Figure 14). The number of Vav1-Cre+;EGFP+ cells at P0 remained constant throughout the time points examined, and only appeared to decrease with passage. The same statistically significant relationship was observed between cells that had been passaged once versus cells that had been passaged twice (P2) showing that P1 cultures contained higher numbers of Vav1-Cre+;EGFP+ per HPF than cells that had been passaged twice. As was seen in P0, the number of Vav1-Cre+;EGFP+ cells remained fairly constant within passage, and only decreased after passaging. Additionally, when viewed under the fluorescent microscope, most of the Vav1-Cre+;EGFP+ cells have the spindle-like appearance traditionally associated with fibroblasts. Of note, when observing the cultures under fluorescent microscopy, Vav1-EGFP- cells (red) are difficult to count, and appear very spread and nearly confluent, despite having a fairly standard shape under phase microscopy.

To further examine the relationship between Vav1-Cre+;EGFP+ cells and passaging in fibroblast growth conditions, a flow cytometric analysis of these cells was performed at the indicated passages to examine if the same trend could be observed (Figure 15). Indeed, at P0 high levels of Vav1-Cre+;EGFP+ cells were detected in fibroblast cultures, while similar results were obtained using CD45 instead of Vav1-EGFP. The percentage of Vav1-Cre+;EGFP+ cells or CD45+ cells significantly

decreased from P0 to P1. This same trend in Vav1-Cre+;EGFP+ cells or CD45+ cells was seen between P1 to P2, with almost no Vav1-Cre+;EGFP+/CD45+ cells observed by flow cytometry. These observations suggest that Vav1-EGFP- "resident" fibroblast may be more effective and efficient at establishing a presence on tissue culture plastic after isolation from lung tissue potentially through an enhanced ability to spread on TC plastic (see Figure 14, P1 and P2). The fibroblast cultures were additionally stained for Col I and examined at P0, P1, and P2 to see if Col I levels were affected by the presence or absence of Vav1-Cre+;EGFP+/CD45+ cells in cultures. No differences were observed between any of the passages examined, indicating that Vav1-Cre+;EGFP+/CD45+ cells contribute to the same level of collagen as do "resident" fibroblasts. These data demonstrate that cells from the hematopoietic lineage can grow under typical fibroblast culture conditions, but their numbers significantly decrease with passage. This observation may be one explanation for why the contribution of hematopoietic cells to fibroblast populations historically has been overlooked.

To evaluate the growth of Vav1+ cells in the absence of Vav1- cells, an additional experiment was performed in which total lung cells isolated from bleomycin and saline-treated mice were incubated with anti- CD45 magnetic microbeads (MACS Miltenyi Biotec), and positively selected using a magnet. The positively selected CD45+ populations were then plated under standard fibroblast conditions as described above. Neither saline nor bleomycin cultures had any meaningful growth by 10 days, and the experiment was stopped (data not shown). These experiments suggest that fibrocytes (CD45+/Col I+) need some type of stimulation from resident cells.

**Low Seeding Densities Yield Fibroblast Cultures of Primarily Vav1-Cre+;EGFP+ Cells**

To assess whether reducing the competition for space between Vav1-Cre+;EGFP+ cells and resident fibroblasts allowed for improved growth of Vav1-Cre+;EGFP+ fibroblasts, experiments were performed using low seeding densities. Total lung cells isolated from saline and bleomycin-treated mice were seeded in either T-25 flasks at $0.35 \times 10^6$ or in 6 well plates at a concentration of $0.15 \times 10^6$, and allowed to attach overnight, while non-adherent cells were washed off the following day. The cell cultures were examined and photographed daily for growth under the fluorescent microscope, and selected time points are shown in Figure 16. Both saline and bleomycin-treated cells exhibited a similar pattern of growth. By seeding the cells at lower densities, fibroblast cultures that were primarily EGFP+ were observed, and this phenotype was maintained until confluency. A phase contrast photo of the cultures at day 14 was included to show that the EGFP+ cells exhibited a typical spindle-like fibroblast shape. These data further suggest that cells from the hematopoietic lineage can differentiate into fibroblasts, and that previous studies may have overlooked their contributions to the fibroblast/myofibroblast populations due to the use of traditional fibroblast culture protocols.

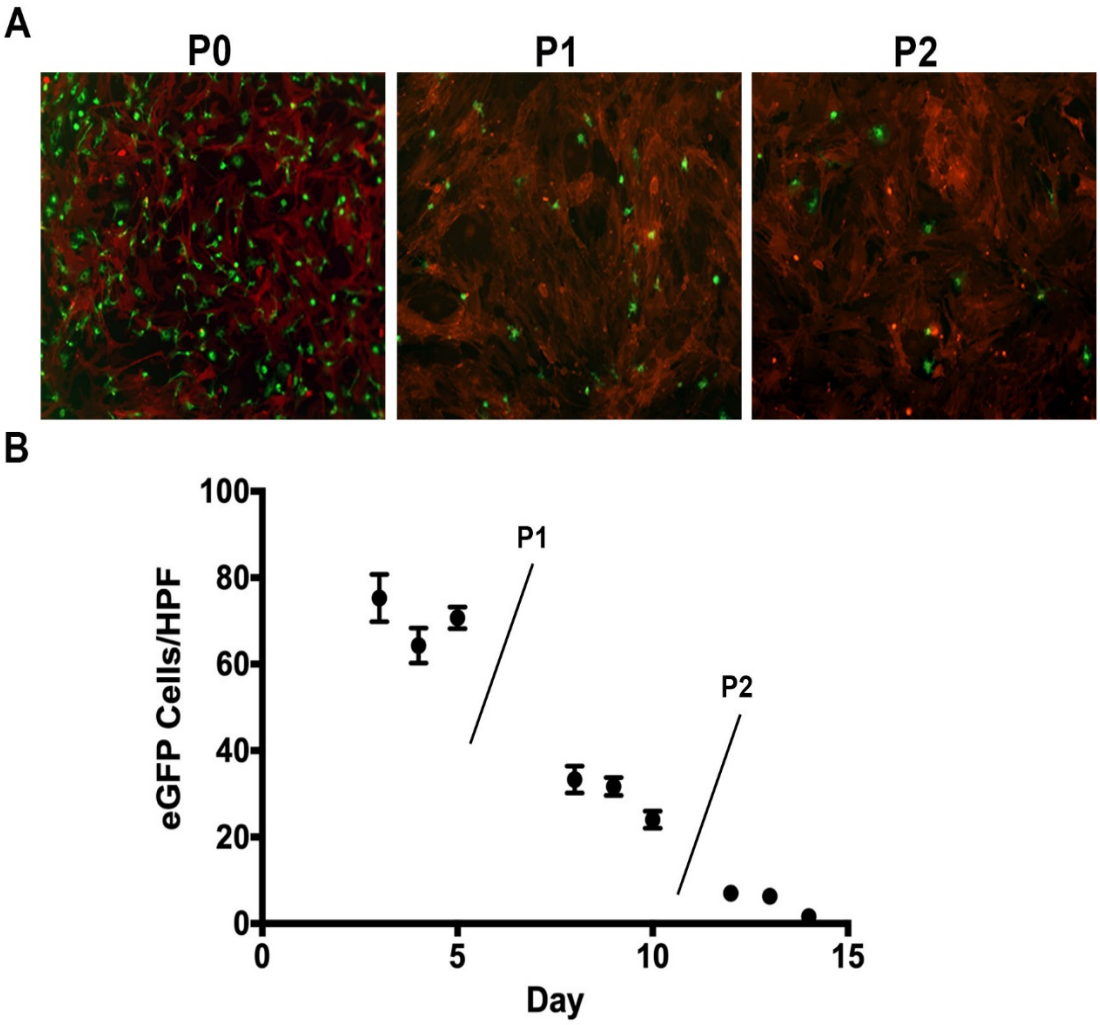


**Figure 14. Vav1-EGFP Fibroblasts decrease with passage.** To assess if cells with a hematopoietic lineage can be grown and contribute to the fibroblast population, total lung cells were isolated from Vav1-Cre;mTmG mice and grown under typical fibroblast conditions. (10% FBS+DMEM, 37°C, and 5% $CO_2$) **(A)** Using a fluorescent microscope, photographs of the fibroblasts were taken at various time points, and a representative HPF was chosen showing a decrease in the number of Vav1-Cre+;EGFP+ cells with passage. **(B)** A quantification of the 3 randomly selected HPFs at the indicated time points, revealing a significant decrease in the number of Vav1-Cre+;EGFP+ between P0 to P1 ($p < 0.01$), and between P1 to P2 ($p < 0.01$).

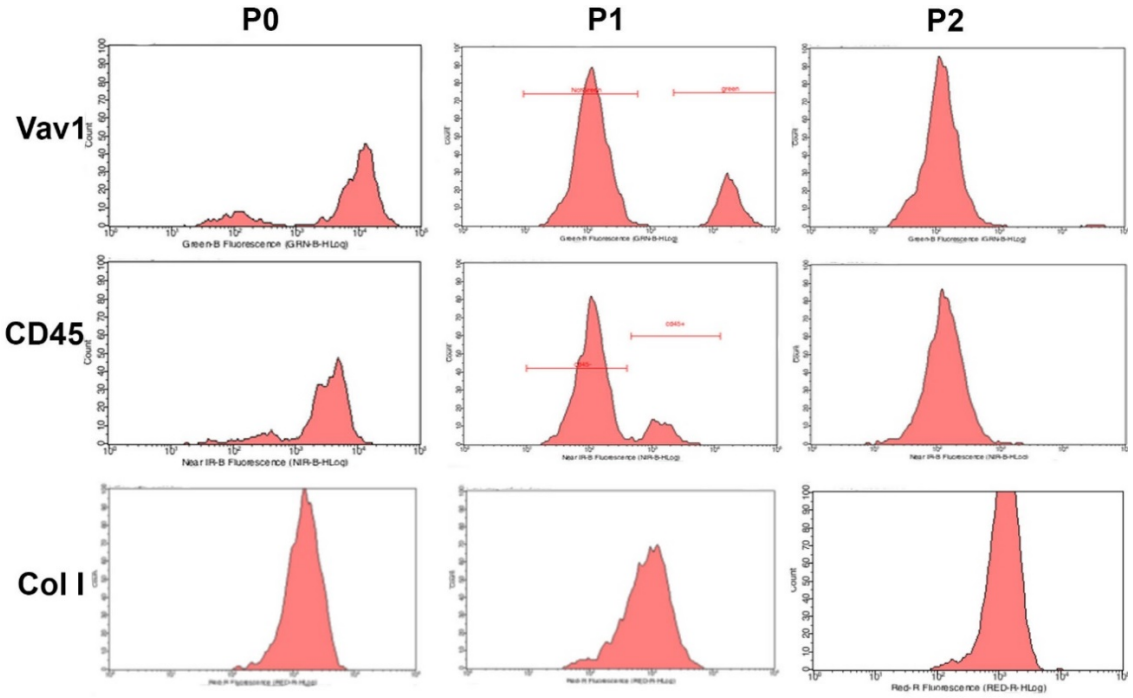


**Figure 15. Vav1-EGFP and CD45 Levels Decrease at the Same Rate With Passage.** To further validate the observation seen in Figure 14, fibroblast cultures isolated from Vav1-Cre;mTmG mice as described above, were collected by accutase, washed, and then labeled with an antibody for CD45 and Col I. This was done during P0, P1, and P2. At P0, high levels of Vav1-Cre+;EGFP+ and CD45+ cells were observed in similar numbers. After one passage, there was a significant decrease in both the levels of Vav1-Cre+;EGFP+ and CD45+ cells as seen by the shift in the peak from the right to the left. By the second passage, almost no EGFP+ and CD45+ cells were found in the fibroblast cultures. Col I staining at all three passages shows that Col I levels were similarly high at P0 when the cultures were heavily Vav1-Cre+;EGFP+/CD45+, and at later passages when Vav-EGFP+/CD45+ levels had fallen. This experiment further validates the observations that Vav1 and CD45 label the same cell populations, that these Vav1-Cre+;EGFP+/CD45+ fibrocytes express Col I at levels similar to Vav1-EGFP-/CD45- resident fibroblasts, and that these cells while initially dominant in fibroblast cultures, decrease over time.

**Growth of Vav1-Cre+;EGFP+ Fibroblasts from BAL**

Because CD45+/Col I+ cells were also observed in the BAL collected from bleomycin and saline-treated mice (Figure 10), experiments was performed to see if cells from the BAL could be grown into typical fibroblast cultures. BAL fluid was collected

from both bleomycin and saline-treated mice and plated at 0.2 x $10^6$ cells per well in a 6 well plate, after overnight culture, unbound cells were removed by washing. The BAL cells were cultured in three different growth conditions: 1. standard fibroblast growth conditions (DMEM+10% FBS) 2. fibroblast conditioned medium (DMEM+10% FBS from overnight fibroblast cultures) 3. co-cultured on pre-existing attached Vav1-EGFP-(red) fibroblasts at about 60-70% confluency. The BAL cultures were observed and photographed daily using a fluorescent microscope to monitor for growth. In the control or standard growth conditions, there was little to no growth throughout all the time points analyzed (Figure 17). The BAL cells grown in conditioned medium,

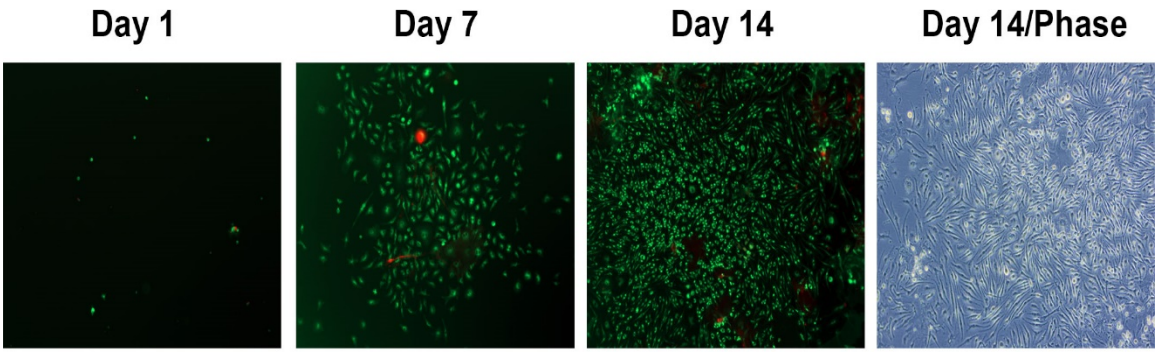


**Figure 16. Low Seeding Density Yields Primarily Vav1-EGP+ Fibroblast Cultures.**

Total lung cells from both saline and bleomycin-treated mice were isolated 21 days post pump implantation, and plated at low seeding densities to reduce competition for space and allowed to grow. For 6-well plates, a seeding density of 0.15 x $10^6$ was used, and for T-25 flasks, a seeding density of 0.35 x $10^6$ was used. The fibroblast cultures were photographed daily using a fluorescent microscope and the growth of Vav1-EGP+ cells was monitored, similar results were obtained for cultures from both saline and bleomycin-treated populations. By Day 14, both the plates and flasks had reached near confluency and were composed of mostly Vav1-EGP+ cells. These cells also exhibited long spindle like shapes typical of fibroblast cultures, and is shown in the Day 14/Phase photo.

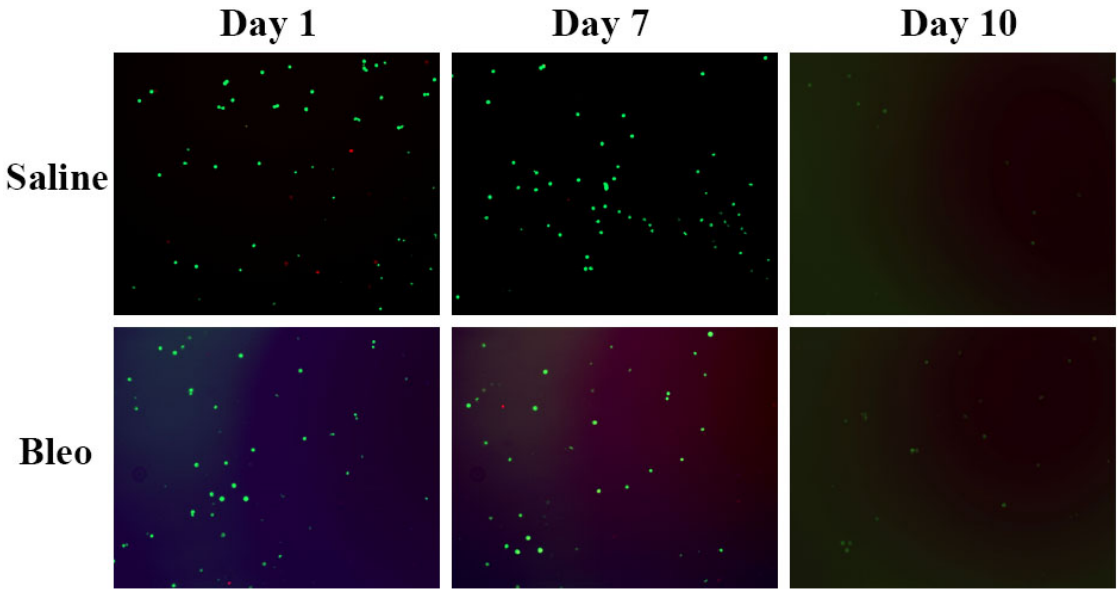


**Figure 17. Growth of Vav1-Cre+;EGFP+ Cells from BAL in Control Conditions.** BAL was isolated from saline and bleomycin-treated mice 21 days post pump implantation, and were plated at 0.2 x $10^6$ cells per well in a 6 well plate using standard fibroblast growth conditions (10% FBS+DMEM, 37°C, and 5% $CO_2$). Cells were observed and photographed daily using a fluorescent microscope, and no growth of cells was observed through all the time points checked.

showed some growth throughout the course of the experiment, but they ultimately failed to fully expand and differentiate into fibroblast-like cells (Figure 18). The BAL cells that were co-cultured on Vav1-EGFP- fibroblasts were able to expand and differentiate into spindle-shaped fibroblast like cells (Figure 19). Both saline and bleomycin-treated BAL cells gave the same results in culture, the only difference observed was in the total number of cells harvested from BAL, with bleomycin-treated BAL containing 3x as many cells as BAL from saline-treated mice. These experiments highlight the idea that while cells from the hematopoietic lineage can differentiate into fibroblasts, they need additional stimulation from resident cells to grow and differentiate. While secreted growth factors may aid in the CD45+ fibroblasts ability to grow, it appears that secreted

factors may be insufficient on their own, and that CD45+ fibroblasts require some type of cell to cell contact for enhanced growth and differentiation.

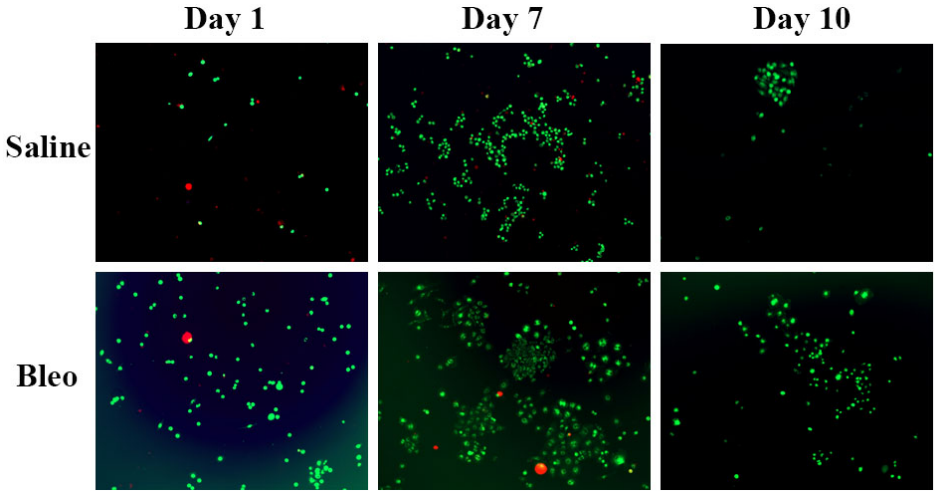


**Figure 18. Growth of Vav1-Cre+;EGFP+ Cells from BAL in Conditioned Medium.** BAL was isolated from saline and bleomycin-treated mice 21 days post pump implantation, and were plated at 0.2 x $10^6$ cells per well in a 6 well plate using conditioned fibroblast growth media (10% FBS+DMEM, 37°C, and 5% $CO_2$ collected from fibroblast cultures after overnight culture). Cells were observed and photographed daily using a fluorescent microscope, cells from both saline and bleomycin-treated mice exhibited some growth and expansion by day 7, but ultimately failed to expand and were dying out by day 10.

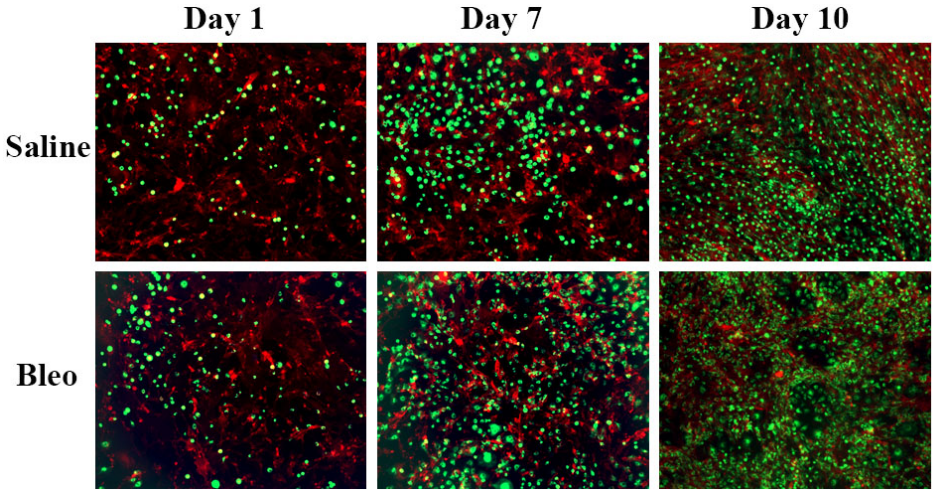


**Figure 19. Growth of Vav1-Cre+;EGFP+ Cells from BAL in Co-Culture Growth Conditions.** BAL was isolated from saline and bleomycin-treated mice 21 days post

pump implantation, and were plated at 0.2 x $10^6$ cells per well in a 6 well plate containing Vav1-EGFP- fibroblasts (red only) at 60-70% confluency, using standard fibroblast growth media (10% FBS+DMEM, 37°C, and 5% $CO_2$). Cells were observed and photographed daily using a fluorescent microscope, cells from both saline and bleomycin-treated mice had higher rates of attachment seen on day 1 than in either control or conditioned medium. Furthermore, Vav1-Cre+;EGFP+ cells from both saline and bleomycin-treated were able to expand and differentiate into spindle-shaped fibroblast like cells.

**Comparing the Adhesion Ability of Vav1-EGP+ Cells with Vav1-EGP- Cells**

To compare the adhesion ability of Vav1-Cre+;EGFP+ cells to Vav1-EGFP- cells, a series of experiments was performed using P0 fibroblasts isolated from Vav1-Cre;mTmG mice (n=3). To perform these experiments, cells were first lifted using accutase, washed, resuspended in DMEM/HEPES, and plated into 96-well plates that were pre-coated with fibronectin at either 0, 1, 3, 10, and 30 µg/ml (Figure 20A). The cells were then incubated for 1 hour at 37°C, before being fixed and washed for observation on a fluorescent microscope. The images were quantified using ImageJ and results are reported as Percent Area (Figure 20C). At 0 µg/ml, non-specific attachment in the absence of fibronectin for both populations was low. Adhesion of the Vav1-Cre+;EGFP+ (green) cells to fibronectin coated wells was nearly maximal at 1 µg/ml. In contrast, Vav1-EGPF- (red) cell adhesion continued to increase up to the highest fibronectin concentration of 30 µg/ml. Put another way, the Vav1-Cre+;EGFP+ (green) cell adhesion was 90% as much at 1 µg/ml fibronectin compared to 30 µg/ml, while Vav1-EGFP- (red) was only 20% as much. These data support the idea that hematopoietic lineage derived fibroblasts are highly responsive to ECM proteins like fibronectin that promote cell adhesion, growth, and differentiation (Klecker and Nair 2017).

**Suppression of Fibrosis in vivo by a Novel Version of CSD**

The caveolin-1 derived peptide, CSD, has been shown to be effective at inhibiting fibrosis in several studies (Tourkina, Richard et al. 2008, Lee, Perry et al. 2014, Reese, Perry et al. 2014). Recently, we have developed a version of CSD better suited for drug development because it is water-soluble. Here we studied how water-soluble CSD (WCSD) would affect hematopoietic lineage derived fibroblast accumulation and fibrosis progression in bleomycin treated mice. As described in the methods, mice were treated with vehicle or bleomycin delivered over seven days by subcutaneously implanted osmotic minipumps. There were three groups of mice: saline treated mice (n=4), bleomycin-treated mice that received vehicle for two weeks starting on day 8 (n=4), and bleomycin-treated mice that received WCSD for two weeks starting on day 8 (n=4). Mice were sacrificed after 21 days, and BAL, lung, and skin tissues were collected. To assess whether WCSD had an effect on fibrocyte accumulation in the lung, total lung cells were isolated and stained with antibodies for CD45 and Col I, and flow cytometry was performed using the Guava easyCyte 8HT. The saline treated mice showed a low amount of fibrocyte accumulation in their lung as expected. Bleomycin-treated mice that received WCSD showed >80% reduction of fibrocyte accumulation compared to mice that received vehicle injections (Figure 21AB). Nevertheless, WCSD had little or no effect on fibrocyte phenotype in terms of other monocyte/macrophage (CD11b, CD68, CD206) and fibrosis markers (α-sma, HSP47, Col I) (not shown). The BAL from these mice was also assessed for fibrocyte accumulation, but no differences were found in the percent fibrocytes between vehicle and WCSD-treated mice (not shown). However, there was a

slight reduction ~(15%) in the total number of cells collected from BAL of WCSD-treated mice compared to the vehicle-treated mice. These data suggest that WCSD is an

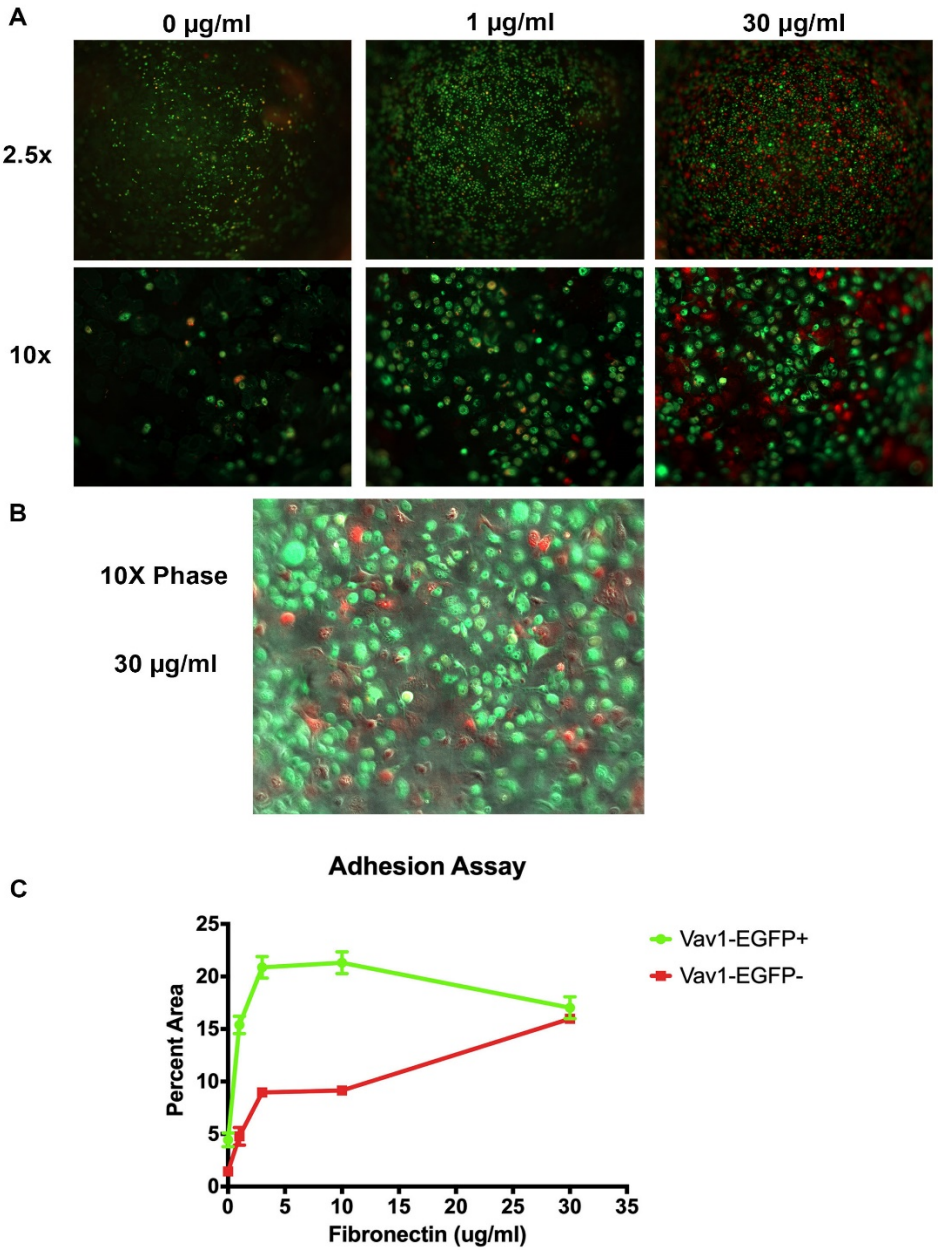


**Figure 20. Adhesion to Fibronectin of Vav1-EGFP- and Vav1-Cre+;EGFP+ Fibroblasts. (A)** Unpassaged fibroblasts from Vav1-Cre;mTmG mice (n=3) were collected using accutase to preserve cell surface receptors, before being plated in 96-well plates that were precoated with fibronectin at concentrations of 0, 1, 3, 10, and 30 µg/ml.

After a 1 hour incubation at 37°C, the cells were fixed and gently washed before being observed and photographed on a fluorescent microscope. Representative photos at 2.5x and 10x magnification are shown, **(B)** with a phase contrast image to demonstrate cell shape. **(C)** Quantification of the Percent Area occupied of Vav1-Cre+;EGFP+ (green) and Vav1-EGFP- (red) cells using ImageJ software. Percent area is shown in terms of the average ± SD of each of 3 saline and 3 bleomycin samples.

effective inhibitor of the accumulation of fibrocytes in the lung tissue, though there was no effect of WCSD on the percent of fibrocytes in the BAL except in the reduction of the total number of BAL cells collected.

In histological studies, lung tissue from vehicle showed very high levels of collagen deposition and inflammatory cell infiltration, while lung tissue from WCSD treated mice were close in appearance to saline-treated mice. Skin tissue from bleomycin/vehicle treated mice showed increased dermal thickening and a near total loss of fat, while skin tissue from WCSD treated mice showed reduced dermal thickening compared to vehicle treated mice, as well as preservation of the fat layer. Overall, the skin from WCSD treated mice had an intermediate phenotype between saline and bleomycin/vehicle treatments. These data indicate that WCSD is effective at mitigating the profibrotic effects of bleomycin in multiple tissues in our mouse model.

To examine the effect of WCSD on the production of proteins associated with fibrosis and with vascular leakage in the lungs of the mice from this experiment, identical lobes were collected from each mouse, homogenized, and extracts were made for Western blot analysis (Figure 22). Prior to analysis, samples were normalized using β-actin to standardize protein loading. For Col I, bleo+veh treated mice had over a three-fold increase in collagen expression compared to saline treated mice, and WCSD treatment reduced collagen expression by about 50%. Bleo+veh treated mice showed a

two and half-fold increase in expression of the myofibroblast marker, alpha-smooth muscle actin (α-sma), compared to samples from saline, and WCSD treatment reduced α-sma expression by 50% in the lungs. Next, tenascin, a protein that is highly expressed during injury and disease was compared between the samples. Bleo+veh saw a six-fold increase in expression of tenascin compared to saline, and WCSD treatment reduced this increase by 50%. HSP47 expression was also examined in these samples due to its importance in collagen production, and as a surrogate marker for myofibroblasts. HSP47

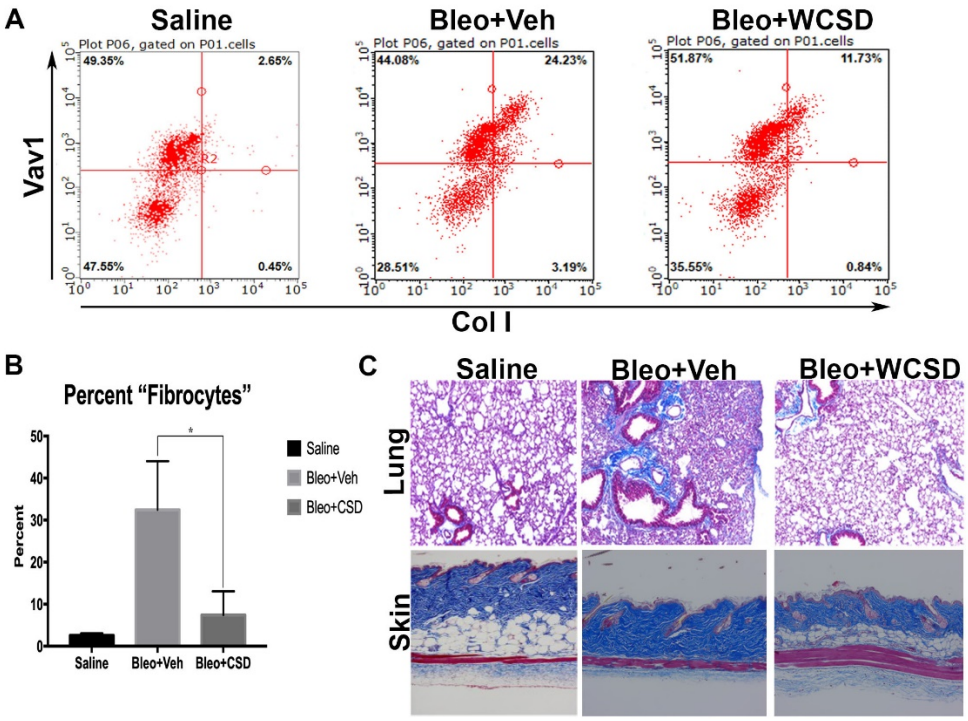


**Figure 21. WCSD Inhibits Fibrocyte Accumulation and Fibrosis in the Bleomycin Mouse. (A)** Total lung cells from saline, bleomycin+vehicle, and bleomycin+WCSD treated mice sacrificed 21 days post pump implantation, and were stained with antibodies for CD45 and Col I. Scatter plots are presented with Vav1 on the y-axis and Col I on the x-axis, CD45 was also analyzed replacing Vav1 on the y-axis and similar results were obtained. **(B)** Perecent fibrocytes (Vav1+/Col I+) are shown as the average ± SD for each of the 4 saline, 4 bleomycin+vehicle, and 4 bleoymycin+WCSD sacrificed 21 days post pump implantation. WCSD significantly inhibited the accumulation of fibrocytes in the lung of bleomycin-treated mice compared to the mice that received vehicle. **(C)**

Representative images from Masson's sections of the lung and skin from saline, bleomycin+vehicle, and bleomycin+WCSD mice. Collagen accumulation was inhibited in the mice that received WCSD compared to the mice that received vehicle in both the lung and skin. WCSD prevented the complete loss of the fat layer in the skin that was seen in the vehicle-treated mouse. *$p < 0.05$

had a seven-fold increase in expression in bleo+veh treated mice compared to saline, and WCSD treatment reduced HSP47 expression by nearly 90%. Lastly, vascular leakage, a hallmark of fibrotic diseases, was examined by looking for IgG leakage into the tissue. The bleo+veh treated lung showed a three-fold increase in the amount of IgG leakage into the tissue compared to saline, and treatment with WCSD reduced this increase by over 100%. Interestingly, the bleo+WCSD was even lower than saline indicating that WCSD treatment is an extremely effective way to prevent vascular leakage. Together these data suggest that WCSD is an effective antifibrotic peptide that both reduces the production of ECM proteins and myofibroblast markers, as well as preventing the accumulation of fibrocytes and other inflammatory cells into the tissue possibly by inhibiting vascular leakage. It is noteworthy that the inhibition by WCSD of fibrocyte accumulation (Figure 21) and the levels of ECM proteins, myofibroblast markers, and vascular leakage were all >50%.

**Human SSc Lung Fibrocytes**

To evaluate if CD45+/Col I+ cells could be found in human lung tissue, a lung tissue sample from a patient diagnosed with SSc was obtained and processed for flow cytometry by using the methods described above. Briefly, the lung tissue was digested with collagenase and a single cell suspension was stained with antibodies for CD45, as well as several other antibodies for monocyte/macrophages and fibrosis. Unstained cells

and CD45+ only labeled cells were used to establish the gating strategy (Figure 23a). A cut-off of 1 x $10^2$ marks the maximum value of fluorescence intensity detected for unstained cells. The addition of CD45 antibody did not change the 1 x $10^2$ cut-off for the fluorescent channel (AF647) of the monocyte/macrophage and fibrosis markers used in

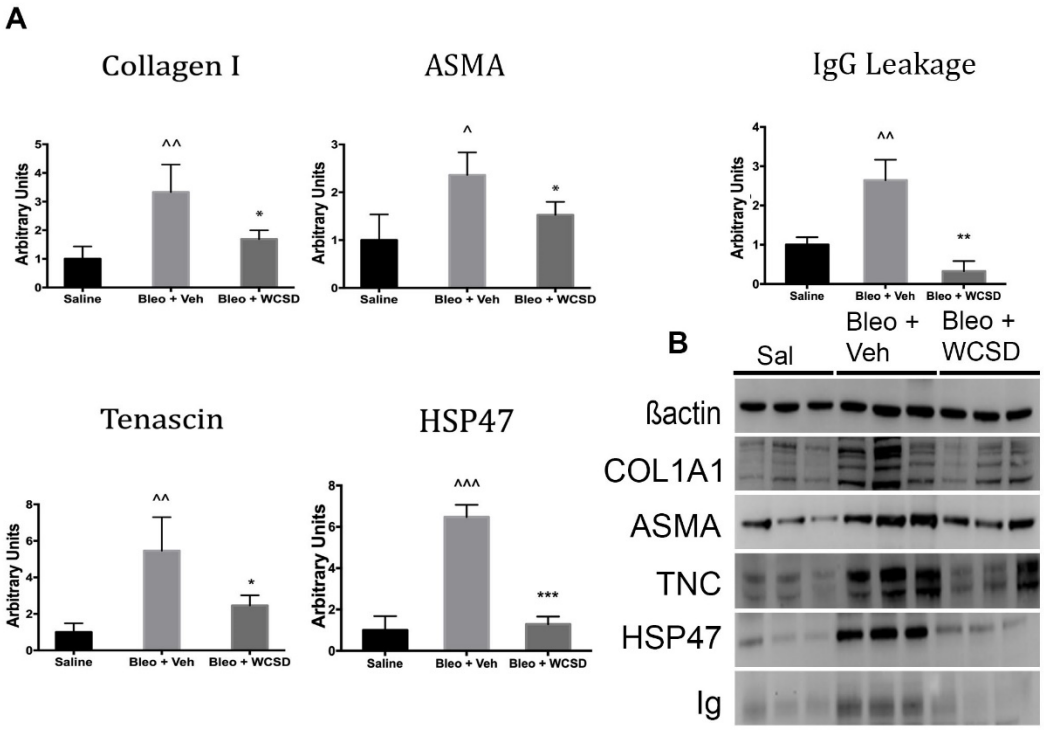


**Figure 22. WCSD Inhibits Fibrosis and Vascular Leakage in the Lung of Bleomcyin-Treated Mice. (A)** Lung tissue from saline, bleomycin+vehicle, and bleomycin+WCSD mice was collected and proteins were extracted for Western Blotting, and then stained with antibodies for fibrosis (Col I, α-sma, Tenascin, HSP47) and for vascular leakage (mouse IgG). Results are shown as a densitometric quantification (average ± SD) normalized against β-actin**.** Densitometric quantification was done using imageJ software. **(B)** Western blot data is shown for all antibodies used. For comparisons of saline vs bleo+veh, *^p < 0.05, ^^p < 0.01, ^^^p < 0.001*. For comparisons of bleo+veh vs bleo+WCSD, **p < 0.05, **p < 0.01, ***p < 0.001*.

this experiment. As expected CD45+ cells were positive for CD68 and Cd206, while CD45- cells were negative for these monocyte markers. In strong support of our

hypothesis that fibrocytes play an important role in fibrotic disease, the levels of Col I, α-sma, and HSP47 were at least as high in CD45+ cells as in CD45- cells. The data from this experiment supports the idea that fibrocytes can be found in the lung tissue of patients with SSc, that the levels of fibrosis markers are as high or higher in CD45+ cells than in Cd45- cells, and these human fibrocytes express similar phenotypes to the fibrocytes detected in the bleomycin-induced fibrosis model for mice.

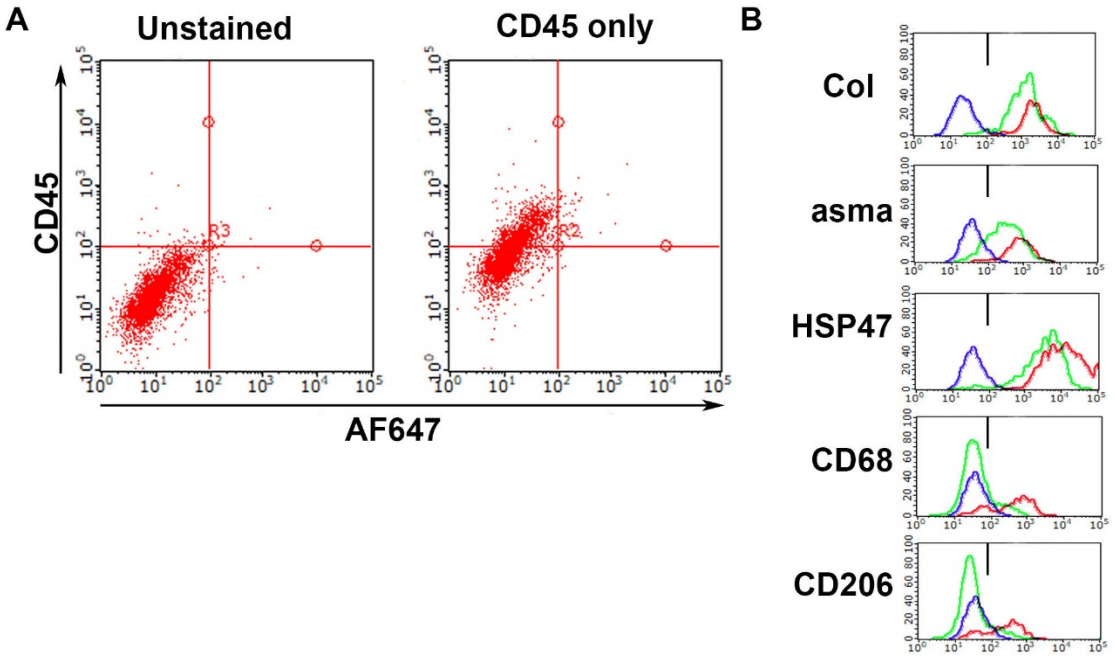


**Figure 23. Human Lung Tissue from SSc Patient Contains Fibrocytes. (A)** Total lung cells from a patient with SSc were left unstained or immunolabeled for CD45 to setup the gating strategy for further characterization with antibodies labeled with AF647. A cut-off of 1 x $10^2$ marks the maximum value of fluorescent intensity for CD45 (y-axis) and AF647 (x-axis). Scatter plots of unstained and CD45 only are shown to validate the gating strategy. **(B)** Total lung cells were labeled with antibodies for CD45, for fibrosis (Col I, α-sma, HSP47), and for additional monocyte/macrophage lineage markers (CD68, CD206) and plotted for MFI positivity. Plots from unstained cells are shown as blue, while 1D plots from the referenced antibodies are shown as green for CD45- cells, and red for CD45+ cells. CD45+ cells from the lung of an SSc patient contained high levels of expression for Col I, α-sma, HSP47, CD68, and CD206, compared to CD45- cells.

**Single-Cell RNA Sequencing of Primary Adherent Cells from Saline- and Bleomycin-Treated Lungs**

To demonstrate by yet another independent method that cells can co-express monocyte markers and fibrosis markers, we performed single-cell RNA sequencing. Unpassaged fibroblast cultures isolated from saline (n=3) and bleomycin-treated (n=3) Vav1-Cre;mTmG mice were allowed to grow to near confluency before being collected with accutase and prepared for single-cell sequencing as described in the methods. Using Partek software, doublets and unlabeled cells were filtered out of the analysis, and the remaining single cell populations from bleomycin and saline fibroblast cultures were processed. By applying dimension reduction to the data through the use of principle component analysis (PCA) and then uniform manifold approximation and projection (UMAP), the data were segregated into 4 distinct clusters shown in Figure 24. By looking at the gene expression profiles of the 4 clusters, we were able to further characterize these clusters and define the groups as: Cluster 1, contained high GFP (monocyte marker) expression and modest Col I expression; Cluster 2, contained moderately high GFP (monocyte marker) expression and high Col I expression; Cluster 3 contained modest GFP (monocyte marker) expression and high Col I; and Cluster 4 contained modest GFP (monocyte marker) expression, modest Col I expression and high levels of endothelial markers (Table 1). Interestingly, as summarized in Table 1, almost all genes that are related to fibroblast activation (vimentin, s1000a4 (FSP1), ACTA2 (α-SMA), Col1a1, Tagln, Tagln2, and Fn1) were expressed in a high percentage of the cells in all 4 clusters. Additionally, certain genes characteristic of monocytes/macrophages were found in

similarly high levels in all 4 clusters, (LGALS3(Mac-3) and LAMP2(Mac-2)). These observations demonstrate the prevalence of cells that express both fibrosis markers and monocyte markers in our cultures.

Cluster 4 was of interest because almost all cells in this cluster when derived from control, saline-treated mice, contained high levels of three endothelial markers (PECAM, Claudin5, LYVE-1). Interestingly, when derived from bleomycin-treated mice, the percentage of cells in this cluster increased 3-fold, PECAM continued to be express at high levels, but the percentage of Cluadin5- and LYVE-1-positive cells decreased drastically. These observations suggest that endothelial-mesenchymal transformation is associated with fibrosis and that this transformation involves the loss of certain endothelial markers. In particular the loss of the tight junction protein claudin5 is likely to result in the enhanced vascular leakage that we observed in bleomycin-treated mice.

While most genes were expressed at similar levels in cells from saline- and bleomycin-treated mice, we noted some other interesting counter-examples besides Claudin5. MMP9 was greatly decreased in expression in cells from bleomycin-treated mice, raising the possibility that the increased level of collagen in fibrotic disease may result in part from decreased degradation. Contrary to expectations based on protein levels, caveolin-1 message is present at increased levels in cells from bleomycin-treated mice. This may be due to cells trying to compensate for low caveolin-1 protein levels by expressing increased levels of message. In any case, it remains to be demonstrated whether this effect occurs in vivo or only in culture.

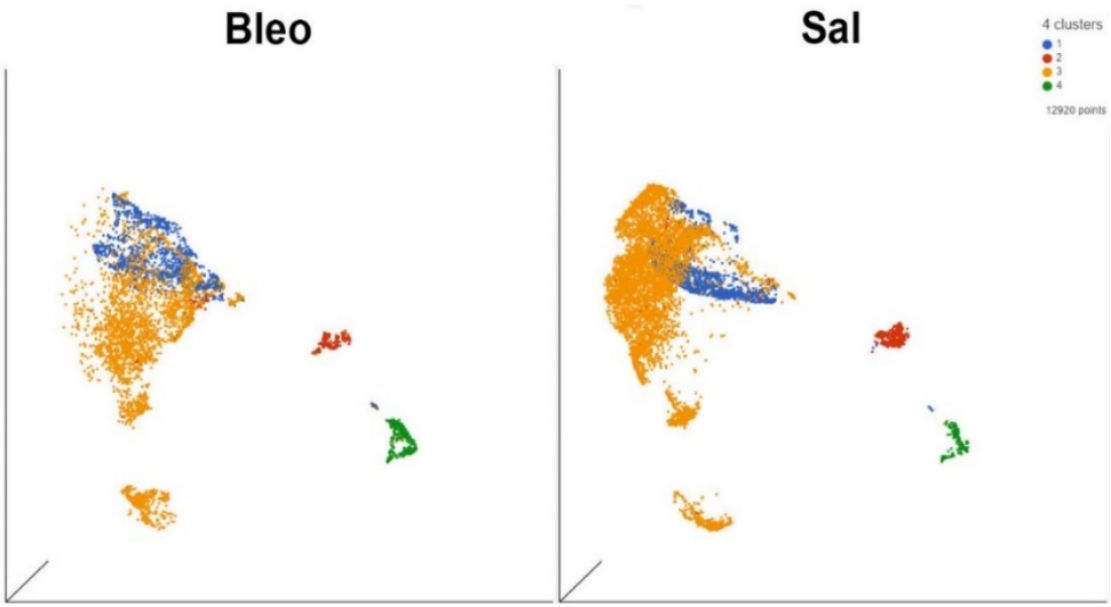


**Figure 24. UMAP Analysis of Fibroblasts Isolated from Bleomycin and Saline-Treated Mice.** The UMAP projection of the fibroblasts isolated from both bleomycin and saline-treated mice is shown. The cells were grouped into 4 clusters using Partek software to apply dimension reduction to data. The clusters are defined as, Cluster 1 (blue), Cluster 2 (red), Cluster 3 (orange), and Cluster 4 (green).

**Table 1. Summary of Single Cell RNA Sequencing Data.** In this table, data are shown as the percentage of cells positive for fibroblast activation, monocyte, endothelial, and selected markers of interest gene expression. Genes expressed in ≥26% in all clusters are highlighted in yellow. *- = 0-5%, + = 6-25%, ++ = 26-50%, +++ = 51-100%.*

| | Cluster 1 | | Cluster 2 | | Cluster 3 | | Cluster 4 | |
|---|---|---|---|---|---|---|---|---|
| | Bleo | Sal | Bleo | Sal | Bleo | Sal | Bleo | Sal |
| **Fibroblast Activation** | | | | | | | | |
| Vimentin | +++ | +++ | +++ | +++ | +++ | +++ | +++ | +++ |
| S100a4 (FSP1) | +++ | +++ | +++ | +++ | +++ | +++ | +++ | +++ |
| FAP | - | - | + | ++ | + | ++ | - | - |
| Serpinh1 (HSP47) | + | ++ | +++ | +++ | +++ | +++ | +++ | +++ |
| ACTA2 (aSMA) | +++ | +++ | +++ | +++ | +++ | +++ | +++ | +++ |
| Col1a1 | ++ | ++ | +++ | +++ | +++ | +++ | ++ | +++ |
| Tagln | +++ | +++ | +++ | +++ | +++ | +++ | +++ | +++ |
| Tagln2 | +++ | +++ | +++ | +++ | +++ | +++ | +++ | +++ |
| DDR2 | - | - | +++ | +++ | +++ | +++ | + | + |
| Fn1 | +++ | +++ | +++ | +++ | +++ | +++ | +++ | +++ |
| **Monocyte** | | | | | | | | |
| CD68 | +++ | +++ | +++ | +++ | + | + | + | + |
| MRC1 (CD206) | +++ | +++ | +++ | +++ | + | + | - | - |
| GFP | +++ | ++ | +++ | +++ | ++ | + | ++ | + |
| PTPRC (CD45) | +++ | +++ | +++ | +++ | - | - | - | - |
| FCGR3 (CD16) | +++ | +++ | +++ | +++ | + | + | - | + |
| CSF1R | +++ | +++ | +++ | +++ | ++ | ++ | - | - |
| F4/80 (ADGRE1) | +++ | +++ | +++ | +++ | - | - | - | - |
| CD11b (ITGAM) | +++ | +++ | +++ | +++ | - | - | - | - |
| LGALS3 (Mac-2) | +++ | +++ | +++ | +++ | ++ | ++ | +++ | +++ |
| LAMP2 (Mac-3) | +++ | +++ | +++ | +++ | +++ | +++ | +++ | +++ |
| **Endothelial Markers** | | | | | | | | |
| PECAM | - | - | - | - | - | - | +++ | +++ |
| Claudin5 | - | - | - | - | - | - | + | +++ |
| LYVE1 | - | - | - | - | - | - | + | +++ |
| **Markers of Interest** | | | | | | | | |
| MMP9 | + | +++ | + | +++ | - | - | - | - |
| Caveolin-1 | + | - | +++ | ++ | +++ | ++ | +++ | +++ |

## Discussion

The contribution of CD45+ cells to primary fibroblasts has been controversial (Kleaveland, Velikoff et al. 2014, Moore-Morris, Guimaraes-Camboa et al. 2014). To evaluate whether cells from the hematopoietic lineage (CD45+) can contribute to the population of fibroblasts in fibrosis, we have used multiple complementary systems and methods to study the levels and phenotypes of CD45+ cells from the fibrotic lung. Systems used include a bone marrow transplant and transgenic mouse models, as well as human lung tissue from a patient with scleroderma-associated ILD. Methods used include flow cytometry and single cell RNA sequencing. All these studies support the concept that CD45+/Col I+ fibroblasts exist and play a central role in fibrotic lung disease, and resolve the issues surrounding fibrocytes by using novel methods to confirm their lineage and contribution to lung fibrosis. We find that:

- CD45+/Col I+ cells (fibrocytes) increase in number and level of Col during fibrosis both in the lung tissue and in the BAL
- The appearance of Col I+ in CD45+ precursors occurs after their recruitment into the lungs
- The fibrocytes express higher levels of monocyte/macrophage markers (CD45, CD16, CD68, CD206) than do CD45+/Col I- cells. They also express high levels of myofibroblast markers ASMA and HSP47.

- CD45+/Col I+ cells are at first predominant in fibroblast cultures (we define fibroblasts as cells that bind to tissue-culture plastic, express Col I, and are spindle-shaped in vitro), but then are lost progressively during passage
    - CD45-/Col I+ cells spread more than fibrocytes and thus may crowd them out despite the fact that fibrocytes can adhere to fibronectin-coated surfaces at lower fibronectin concentrations
    - Fibrocytes do not appear to grow in vitro in the absence of CD45-/Col I+ cells
- Treatment with a novel, water-soluble version of CSD called WCSD inhibits fibrocyte accumulation as well as overall Col, Tenascin C, α-sma, and HSP47 levels and vascular leakage. The decreased fibrocyte accumulation may result both from decreased precursor recruitment due to decreased vascular leakage and to the decreased differentiation of fibrocytes from CD45+/Col I- precursor monocytes.
- WCSD also reverses the pathological effects of systemic bleomycin on the loss of the transdermal adipose layer.

**Identification and Characterization of CD45+ Fibroblasts**

To recapitulate the features of ILD seen in patients with SSc or IPF, an animal model in which bleomycin is delivered systemically via osmotic minipumps (Lee, Reese et al. 2014) was used to more accurately model the effects of the disease compared to the more routine model where bleomycin is delivered directly into the lungs. We find that

there are populations of cells in both control and fibrotic lung tissue that are of hematopoietic origin, and yet express markers for fibrosis such as, Col I and HSP47, as wells as expressing other monocyte macrophage markers including CD11b, CD16, CD68, and CD206. In fibrotic lung tissue, the number of these cells was significantly increased compared to control lung tissue, and these cells derived from the hematopoietic lineage in fibrotic tissue also expressed higher levels of collagen.

By looking at the time course for the accumulation of CD45+/Col I+ cells in the fibrotic lung, we confirmed the association of these cells with the development of fibrosis. By breaking CD45+/Col I+ cells into two regions, Region I ($CD45^{high}$/Col I+) and Region II (CD45+/Col I+), we were able to differentiate between the early inflammatory response from pump installation, and the later accumulation of these cells in response to fibrosis. In both saline or bleomycin-treated mice, the number of cells found in Region I (CD45high/Col I+) remained low 3 days after pump implantation. After 10 days, the number of cells in Region I (CD45high/Col I+) remained low in the saline lung, but showed a slight increase in the bleomycin lung. By day 28, the number of cells in Region I (CD45high/Col I+) had dramatically increased in the bleomycin lung while remaining unchanged in saline. The results in Region I (CD45+/Col I+) showed an interesting difference at day 3 compared to what was seen in Region I (CD45high/Col I+). Both saline and bleomycin lung, had large numbers of CD45+/Col I+ cells in Region II 3 days after pump implantation, which decreased significantly by day 10. The number of cells in Region I (CD45+/Col I+) remained relatively unchanged in both saline and bleomycin lung by day 28, but by this time point the number of cells observed in the

bleomycin lung was significantly higher than in the saline lung. Our observations support the idea that CD45+/Col I+ cells (particularly CD45high/Col I+ cells) accumulate in the lung over time, and that an initial transient increase in the number of CD45+/Col I+ cells is likely due to the surgery and pump implantation rather than the contents of the pumps.

Because circulating fibrocytes have been reported in both human disease and various mouse models (Yang, Scott et al. 2002, Galligan and Fish 2012, Russell, Herzog et al. 2012, Lin, Alrbiaan et al. 2020), we investigated whether we could detect these cells among circulating PBMCs in the bleomycin pump model. While we did detect an initial small increase in circulating CD45+/Col I+ cells shortly after pump installation (both vehicle and bleomycin pumps), this increase did not persist, using antibodies for CD45 and Col I, very low levels of fibrocytes were detected in the blood from both saline and bleomycin-treated mice. Interestingly, a similar increase in the number of cells in Region I (CD45+/Col I+) was observed at day 3 for both saline and bleomycin PBMCs, as was the subsequent decrease. These observations further support the idea that there is an early inflammatory response to the implantation of the pump that resolves by day 10. These observations may also suggest that cells of hematopoietic origin may not fully differentiate into fibroblast-like cells until they reach their target tissue. Despite the fact that other studies report finding circulating fibrocytes in the PBMCs of mice (Lin, Alrbiaan et al. 2020), we were unable to detect them even when using several different antibodies for Col I.

Because Col I is a secreted protein that has been reported to be taken up by cells, we performed a wide variety of control experiments to rule out the possibility that the

CD45+/Col I+ cells that we detect picked up Col I from the extracellular matrix in vivo that had been secreted by CD45-/Col I+ cells. First of all, the antibody that we use to detect Col I (which we call Pro) was made against the Col Iα1 C-terminal propeptide. This peptide is cleavage off of Col I prior to its deposition in the extracellular matrix, so should not recognize Col I derived from the extracellular matrix. Next, one would expect Col I derived from the extracellular matrix to be bound to the cell surface. However, we only detected Col I in cells that had been fixed and permeabilized, not in live cells (data not shown). (Fix-permeabilization was also necessary to detect certain other markers that we used; namely the macrophage marker CD68 and the myofibroblast markers HSP47 and ASMA). In another approach, we used the Col I chaperone HSP47, which is involved in the secretion, processing, and stabilization of collagen I (Hagiwara, Iwasaka et al. 2007, Ishida and Nagata 2011) and not present in the extracellular matrix, as a surrogate marker for collagen production. We found that there are significantly higher levels of HSP47 in CD45+/Col I+ cells compared to CD45+/Col I- cells. In addition to this observation, CD45+/Col I+ cells from bleomycin lung contained significantly higher levels of HSP47 than was found in CD45+/Col I+ cells from saline lung. These data are consistent with several studies that demonstrate that HSP47 is upregulated in fibrosis (Kakugawa, Yokota et al. 2013, Lee, Reese et al. 2014, Pleasant-Jenkins, Reese et al. 2017, Miyamura, Sakamoto et al. 2020). Finally, we used transgenic mice that express EGFP under the control of the Col Iα1 promoter. It is straightforward to detect endogenous Col I expression in these mice as EGFP, while adsorbed Col I would not be detected as EGFP. These observations strongly support the idea that BM cells are recruited into sites of fibrosis and are capable of producing their own collagen and

contributing to the population of myofibroblasts in the tissue, and is similar to what has been reported in renal fibrosis (Li, Deane et al. 2007, Jang, Kim et al. 2014, Wang, Meng et al. 2016).

While most of the experiments used in these studies made use of 10 to 12-week old C57BL/6 mice to confirm the presence of CD45+/Col I+ cells in the lungs of fibrotic mice, some of the experiments performed in the study used 24-week old C57BL/6 mice. These mice had undergone irradiation, and received BM transplants from mice that express EGFP in all of their cells. This approach allowed us to see if CD45+/Col I+ cells are in fact BM-derived, and whether the fibrotic response to bleomycin was something that occurred in both young and old mice. These studies confirmed that all CD45+ cells from both saline and bleomycin-treated mice were BM derived, and that CD45- cells did not express EGFP. This study also showed that the strong fibrotic response to bleomycin was not just limited to young mice, but can also occur in mice that are several months older. This observation may be useful as many studies make use of relatively young mice (10 weeks) to study ILD, while most patients that develop ILD are older adults (Foocharoen, Netwijitpan et al. 2016). Additionally, lung tissue sections taken from the bleomycin mice not only showed increases in the number of EGFP+ cells, they also showed that the EGFP+ cells are also positive for Col I. Together these data further support the idea that during fibrosis, CD45+ cells accumulate in the lung tissue and express Col I.

**Lineage Tracing of Vav1 Derived Fibrocytes and Fibroblasts**

By using Vav1-Cre;mTmG mice, we were able to further assess the contribution of hematopoietic cells to the population of fibrocytes and fibroblasts, as well as perform additional experiments to further characterize these cells. Vav1 is expressed early in the development of hematopoietic cells. In our model these cells are marked by their expression of EGFP (Georgiades, Ogilvy et al. 2002). These studies allowed for the monitoring of hematopoietic (Vav1) cells without the use of antibodies, and also for monitoring of live cultures of Vav1+ cells by fluorescent microscopy. As with our previous experiments, we detected significant increases in the number of hematopoietic cells (Vav1-Cre+;EGFP+) that expressed Col I in the lungs of mice that received bleomycin compared with saline-treated mice. The same result was observed whether we used Vav1-EGFP or CD45 double labeled with antibodies for Col I; confirming that Vav1-EGFP expression was a reliable marker for all hematopoietic cells. In addition to looking at total lung cells, BAL was also isolated from both bleomycin and saline-treated mice and the same flow cytometric analyses were performed. As with the total lung cells, there was an increase percentage of Vav1+/Col I+ cells in the BAL from bleomycin lungs compared to saline. In addition to the increased percentage of Vav1+/Col I+ cells, there were three times as many total cells in the BAL of bleomycin-treated mice. This observation is likely due to the increased vascular leakage characteristic of bleomycin treatment and fibrotic diseases like ILD (Swaney, Chapman et al. 2010, Gendron, Lemay et al. 2017, Zhao, Tian et al. 2019). These observations on both total lung cells and BAL cells confirm that Vav1 is a reliable marker for hematopoietic cells that marks the same

population of cells from our experiments that used CD45 or EGFP+ BM cells to identify cells of hematopoietic lineage origin.

To further phenotype the Vav1 cells that contribute to fibrosis, a panel of antibodies for monocyte/macrophage and fibrosis markers was used on cells expressing Vav1-EGFP from total lung digests and BAL from bleomycin and saline-treated mice. In the lungs of bleomycin-treated mice, for the monocyte/macrophage markers we found significant increases in the numbers of cells expressing CD11b, CD16, and CD68 compared to the lungs from saline-treated mice. In cells isolated from the BAL, there were significant increases in the numbers of cells expressing CD11b and CD16 in the bleomycin BAL. These data further confirm that there are increased numbers of monocyte/macrophages in both the lung and BAL of bleomycin treated mice. When the fibrosis markers were analyzed in Vav1-Cre+;EGFP+ cells from bleomycin and saline-treated mice, we found bleomycin-treated mice exhibited significant increases in the number of cells expressing Col I, using antibodies against both the collagen Iα1 C-terminal propeptide and the Collagen Iα1 C-terminal telopeptide in cells from both the lung and BAL of bleomycin. Higher numbers of cells expressing α-SMA and HSP47 were also detected in the bleomycin lung, but the difference was not significant. However, the level of HSP47 in these cells from bleomycin-treated mice was much higher than in saline-treated mice. Together these data indicate that fibrosis is characterized by increased numbers of hematopoietic lineage cells in both the lung and BAL, and that these cells express high levels of fibrosis markers.

Since hematopoietic lineage (Vav1-EGP+) cells were shown to express fibrosis markers, we wanted to determine the contribution these cells would make to fibroblast cultures prepared under routine conditions. In unpassaged fibroblast cultures, there were relatively high numbers of Vav1-Cre+;EGFP+ cells observed by fluorescent microscopy from day 1 (when unbound cells are removed) to confluency for cultures from both bleomycin- and saline-treated mice. The Vav1-Cre+;EGFP+ cells appeared to be smaller in size than the Vav1-EGFP- cells and appeared to be less spread than the Vav1-EGFP- cells. After the fibroblasts reached confluency, the cells were passaged. We noted a dramatic decrease in the number of Vav1-Cre+;EGFP+ cells in the fibroblast cultures. The number of Vav1-Cre+;EGFP+ cells decreased even further after an additional passaging resulting in cultures with almost no Vav1-Cre+;EGFP+ cells. To confirm the visual observations, flow cytometry was performed on the fibroblast cultures at the various passages. Similar high numbers (>75% of total cells) of Vav1-EGP+ or CD45+ cells were observed in unpassaged cells. The decreases in Vav1-Cre+;EGFP+ cells vs passage detected by flow cytometry totally paralleled the decreases observed by fluorescent microscopy. These observations indicate that cells of hematopoietic origin are capable of growing in typical fibroblast cultures, but may ultimately be outcompeted for space by resident fibroblasts due to the enhanced ability of the resident fibroblasts to spread. This observation may be why many researchers have overlooked the contribution of hematopoietic cells to fibroblast populations, as experiments are typically done with fibroblasts that are at least in passage 3.

Since it appears that while fibroblasts derived from the BM can grow in fibroblast cultures, but may be outcompeted for space by resident fibroblasts, experiments were preformed to examine whether BM derived fibroblasts could grow with reduced competition for space. Initially, CD45+ cells were isolated from the lung tissue of both saline and bleomycin-treated mice, but were unable to grow and expand under normal fibroblast conditions. However, when total lung digests were plated at 50% the routine seeding density, the Vav1-Cre+;EGFP+ cells were able to grow and expand to the point that the Vav1-Cre+;EGFP+/Col I+ fibroblasts were >90% of the cells in the culture. These data further support the idea that cells from the hematopoietic lineage contribute to the fibroblast population in vivo and in vitro prior to passage.

To further evaluate whether Vav1-Cre+;EGFP+/Col I+ fibroblasts require Vav1-EGFP-/Col I+ cells to grow, we used BAL cells (>95% CD45+) as the source of Vav1-Cre+;EGFP+/Col I+ fibroblasts. These cells were cultured either using routine fibroblast growth media, conditioned media from Vav1-EGFP- fibroblast cultures, or in co-culture with established cultures of Vav1-EGFP- fibroblasts. These experiments revealed that with no additional stimulation, the CD45+ cells failed to grow and expand in culture; and that CD45+ cells grown in conditioned media had some growth and expansion, but ultimately failed to assume a spindle shape and grow to confluency. It was only in co-culture that the CD45+ cells were able to grow well and uniformly assume a spindle shape. These data support the idea that both secreted factors, ECM proteins, and/or cell contact provided by Vav1-EGFP- fibroblasts may be critical in allowing BM derived cells to grow and assume the spindle shape characteristic of fibroblasts.

The ECM protein fibronectin is upregulated in the lung of many different fibrosis related injuries, and plays a role in the adhesion, activation, and recruitment of fibroblasts in the lung (Roman, Ritzenthaler et al. 2004, Muñoz-Esquerre, Huertas et al. 2015, Klecker and Nair 2017, Ghavami, Yeganeh et al. 2018). For these reasons and because fibronectin is well-known as a protein capable of mediating fibroblast adhesion, we performed an experiment to compare the ability of Vav1-Cre+;EGFP+ and Vav1-EGFP- fibroblasts to adhere to plates coated with fibronectin. Cells harvested from unpassaged fibroblast cultures containing both Vav1-Cre+;EGFP+ and Vav1-EGFP- cells were plated in 96-well plates coated with a range of concentration of fibronectin. Interestingly, at the lowest concentration of fibronectin tested (1 μg/ml in the coating solution), near-maximal attachment of Vav1-Cre+;EGFP+ cells occurred. In contrast, the adhesion of Vav1-EGFP- cells continued to increase up to the highest concentration of fibronectin tested (30 μg/ml in the coating solution). These data suggest that Vav1-Cre+;EGFP+ cells are highly responsive to the ECM protein fibronectin and raise the possibility that in fibrotic diseases the increased concentration of ECM proteins leads to activation of fibroblasts derived from the hematopoietic lineage.

**WCSD Decreases Fibrocyte Levels and Fibrosis in the Bleomycin Lung**

Previous data from our lab has shown that PBMCs from patients with SSc-ILD express lower levels of caveolin-1 than healthy controls, and that the use of a caveolin surrogate peptide, CSD, is effective at blocking the recruitment of these cells towards several chemokines in vitro and their expression of Col I (Reese, Dyer et al. 2013, Lee, Perry et al. 2014, Reese, Perry et al. 2014). In addition, CSD inhibits Col I expression by

myofibroblasts and mesenchymal stem cells (Tourkina2005, Lee2019). To address the importance of fibrocytes in lung fibrosis, a novel water-soluble version of CSD (WCSD) was used to evaluate the effects of the peptide on fibrocyte accumulation and the progression of fibrosis in bleomycin-treated mice. The mice received bleomycin by osmotic minipump for 7 days, at which point the mice were given daily I.P. injections of either WCSD or vehicle until they were sacrificed at day 21. Treatment with WCSD was effective in reducing the number of CD45+/Col I+ cells in the lungs compared with vehicle treated mice, even though treatment with WCSD did not begin until after bleomycin administration had stopped. Our experimental design does not allow us to determine whether WCSD inhibited the recruitment of fibrocyte precursors into the lungs or inhibited the differentiation of the precursors into Col I+ fibrocytes; based on previous studies, however, we expect that WCSD is inhibiting both processes. While WCSD reduced the number of fibrocytes, it did not significantly alter their phenotype.

Additionally, lung and skin tissue were collected from these mice and Masson's trichrome staining was performed. WCSD was effective at inhibiting the amount of inflammation (cellularity) and collagen deposition in the lungs of the bleomycin-treated mice, compared to those that only received vehicle. WCSD also prevented the complete loss of fat in the dermal layer that was seen in mice that only received vehicle treatment. Lung tissue extracts were also examined by Western blot for their expression of ECM proteins associated with fibrosis (Col I, Tenascin C), myofibroblast markers (α-sma, HSP47) (van Amerongen, Bou-Gharios et al. 2008, Hinz, Phan et al. 2012, Cao, Wang et

al. 2018), and for vascular leakage measured by the amount of IgG in the tissue. WCSD almost completely inhibited the over-accumulation in the tissue of all of these proteins.

These major beneficial effects of WCSD on fibrosis may result from the direct inhibition of the expression of Col I, tenascin c, α-sma, and HSP47. They may also result from a decrease in the recruitment of inflammatory cells as a consequence of the inhibition of the vascular leakage known to occur in fibrotic lungs (Tang, Zhao et al. 2014, Gendron, Lemay et al. 2017). It is also possible that inhibiting the expression of certain ECM proteins contributes to the inhibition of the recruitment of inflammatory cells, given that fibronectin and tenascin c have been shown to promote recruitment in fibrosis(Roman, Ritzenthaler et al. 2004, Bhattacharyya, Wang et al. 2016).

In other words, WCSD may be preventing BM derived cells from leaving the circulation and entering the tissue, as well as inhibiting the release of chemo attractants into the circulation. Together, these data strongly support the idea that WCSD is effective at inhibiting the progression of fibrosis by reducing the number of BM derived fibroblasts in the tissue by blocking their recruitment and activation into myofibroblasts.

**CD45+/Col I+ Cells in Human SSc-ILD Lung Tissue**

To address whether fibrocytes (CD45+/Col I+ cells) could be found in the lungs of patients with ILD, lung tissue from a patient with SSc-ILD was analyzed by flow cytometry. These studies revealed a population of fibrocytes from the SSc-ILD lung that were CD45+/Col I+, and these fibrocytes also expressed the monocyte/macrophage markers CD68 and CD206, as well as the myofibroblast markers α-sma and HSP47.

While several other studies have reported detecting fibrocytes in the circulation and BAL of patients with ILD (Fujiwara, Kobayashi et al. 2012, Borie, Quesnel et al. 2013, Sun, Zhu et al. 2016, Wollin, Distler et al. 2019), to the best of our knowledge this is the first report detecting these cells in lung tissue. The data from this experiment show that as in our animal model for ILD, CD45+/Col I+ can be detected in human lung samples, where they appear to be contributing to the population of myofibroblasts.

**Single-Cell Sequencing of Fibroblasts from the Saline and Bleomycin Lung**

The use of single-cell RNA sequencing (scRNA-seq) has become a powerful tool in the understanding of cell functions, responses to treatments, and disease progression at the single-cell level (Gao 2018). To fully characterize and understand the populations of cells that are contributing to the fibroblast populations, we utilized this technique to study fibroblasts that were isolated from both saline and bleomycin-treated Vav1-Cre+/mTmG mice. Total lung cells were first isolated and grown under routine conditions till near confluency before processing for scRNA-seq. By processing the data and applying dimension reduction using PCA and UMAP, we recognized 4 clusters of cells that could be characterized by their gene expression profiles. The cells in Cluster 1 expressed the highest levels of GFP which marks hematopoietic-lineage derived cells, as well as expressing modest levels of Col I. Cluster 2 expressed moderately high levels of GFP, and high levels of Col I. The cells in cluster 3 contained modest levels of GFP and high levels of Col I. The cells in cluster 4 expressed moderate levels of both GFP and Col I, but expressed high levels of endothelial markers. Cells from both saline and bleomycin fell into these clusters, and overall shared fairly similar features.

To further characterize and compare the clusters, we examined several genes associated with fibroblast activation and monocyte markers. Interestingly, there were many genes for fibroblast activation expressed in high levels across all 4 of the clusters. The intermediate filament protein, vimentin, which plays an important role in the migration, growth, and proliferation of fibroblasts, and is associated with their response to injury, was highly expressed in all clusters (Mendez, Restle et al. 2014, Cheng, Shen et al. 2016). FSP1, a protein that is expressed by fibroblasts in tissue remodeling and has also been used to identify fibroblasts that have undergone epithelial to mesenchymal transition (EMT) in different organs, was high in all clusters (Österreicher, Penz-Österreicher et al. 2011). Other genes (α-sma, Col I, Transgelin [Tagln], Tagln2, fibronectin 1 [FN1]} associated with fibroblasts as well as their response to injury were expressed in all four clusters. In summary, all the clusters are composed of cells with a variety of fibroblastic characteristics.

We further examined the 4 clusters for their expression of various hematopoietic lineage and monocyte markers. Most important, while clusters 1 and 2 contained high levels of EGFP, clusters 3 and 4 contained moderate levels of EGFP when derived from saline-treated mice, but contained much higher levels when derived from bleomycin-treated-mice. Certain genes considered to be monocyte markers (Galectin-3 [LGALS3] or Mac-2) and lysosome-associated membrane protein 2 (LAMP2 or Mac-3) were expressed by a high percentage of cells in all 4 clusters. Therefore, it is difficult to simply state that any particular cluster represents fibrocytes and that any particular cluster represents resident fibroblasts(Dong and Colin Hughes 1997, Chueh, Lin et al. 2015). This difficulty

may result from the fact that all of these cells have been removed from the in vivo environment and been cultured on plastic in the presence of 10% serum that may cause a convergence in the phenotypes of fibroblasts from saline- and bleomycin-treated mice. Experiments in which cells are analyzed directly after release from tissue may help overcome this ambiguity. Given these caveats, we believe that the clusters that we have observed for the most part represent: Cluster 1, Fibrocytes; Cluster 2, Myofibroblasts derived from fibrocytes; Cluster 3, Resident fibroblasts; Cluster 4, Cells undergoing endothelial-mesenchymal transformation.

Monocyte markers (e.g., CD68, CD206, GFP, CD45, CD16, Colony Stimulating Factor 1 Receptor [CSFR1], F4/80, and CD11b) are expressed at high levels in clusters 1 and 2. These genes are expressed at moderate levels in clusters 3 and 4, but among this group only GFP was expressed in high levels of cluster 3 and 4, and that was only in cells from the bleomycin-treated mice.

When the 4 clusters were examined for their expression of various endothelial markers, there were no genes expressed by a high percentage of cells across all 4 clusters. In fact, clusters 1-3 contained almost no cells expressing endothelial markers. Platelet endothelial cell adhesion marker (PECAM-1) was the only gene that was expressed in a high number of cells from both bleomycin and saline-treated mice in cluster 4. Claudin and lymphatic vessel endothelial hyaluronic acid receptor 1 (LYVE1) were expressed in cells from both bleomycin and saline mice, but only saline contained high (≥50%) numbers of cells expressing these genes. Studies on whether the loss of the tight junction

protein claudin5 is related to the increase in vascular leakage will be an exciting topic for future research.

Additionally, we examined the expression of matrix metalloproteinase 9 (MMP-9) and Caveolin-1 (cav-1), two genes of interest to this study. MMP-9, expressed by a wide variety of cell types including monocyte/macrophages and fibroblasts, is an interesting molecule that plays a profibrotic part as well as a role in the resolution of fibrosis. This dynamic role of MMP-9 is seemingly temporal, where MMP-9 has been shown to promote a fibrotic response early, while aiding in the resolution of fibrosis at later stages (Feng, Ding et al. 2018, Wang, Gao et al. 2019, Wang, Liu et al. 2019). When we examined our clusters for MMP-9 expression, we found that expression was largely limited to clusters 1 and 2, with little to no expression in clusters 3 and 4. Interestingly, the number of cells expressing MMP-9 was highest in saline for both clusters 1 and 2. This increase in MMP-9 expression in saline cells may reflect the fact that these cells have left an in vivo environment with no fibrotic stimuli, and are now being cultured on tissue culture plastic potentially initiating a fibrotic response in these cells. Conversely, an opposite effect was observed when we looked at cav-1 expression in the 4 clusters. While all clusters had some expression of cav-1, there were only high numbers of cells expressing cav-1 in clusters 2-4. Interestingly, the percentage of cells expressing cav-1 was higher for cells from bleomycin-treated mouse compared to saline in all clusters. This is somewhat unexpected, as previous data from our lab showed that both in the bleomycin animal model and in patients with SSc-ILD, cav-1 expression was decreased in fibrocytes, monocytes, and other fibrosis related cell types (Lee, Reese et al. 2014,

Reese, Perry et al. 2014). However, this observation may reflect the fact that now that these cells are out of the bleomycin/fibrosis environment, they may have increased their expression of cav-1 to make up for any loss that was occurring due to the fibrotic stimuli. These data further suggest that by removing these cells from their in vivo environment and placing them on TC plastic, we are potentially inducing changes to the both the types of cells and their phenotypes that aren't truly reflective of the populations of fibroblasts and fibroblast precursors seen in vivo.

**Summary**

In summary, the results of these studies strongly suggest that during fibrosis cells from the hematopoietic lineage that express Col I and other fibrosis markers increase in number, and that their differentiation into these fibroblast precursors primarily occurs once they are in the target tissue. Previous studies may have overlooked the contributions of these cells to the fibroblast populations, since they disappear from in vitro cultures with passaging and are difficult to detect using IHC. These studies highlight several potential therapeutic targets (using WCSD or other treatments), including the recruitment and differentiation of fibrobcytes, as well as receptors that may interact with ECM proteins like fibronectin to promote adhesion and differentiation of these cells.

**Limitations**

There are several limitations to the experiments performed in this study for a variety of different reasons, and which could be addressed in future experiments. Characterization of the phenotype of hematopoietic derived cells would have benefited

from a more in-depth analysis using the Col-EGFP mice, rather than just the Vav1-Cre/mTmG mice. By using the Col-EGFP mice, we would be able to provide a more precise characterization of CD45+/Col-EGFP+ cells rather than having to rely on Vav1-Cre+;EGFP+ cells for this characterization, or through the use of antibodies for CD45 and Col I. Unfortunately, limited numbers of Col-EGFP mice and equipment failures prevented these analyses for this study. Another area that could benefit from additional investigation would be further expanding the growth conditions for isolated CD45+ and BAL cells in culture. While we identified that hematopoietic cells (Vav1-Cre+;EGFP+) were highly responsive to the ECM protein, fibronectin, and that fibronectin promoted their adhesion, there were no experiments performed to see how fibronectin and other ECM proteins affected the growth of CD45+ or BAL cells isolated from the lung. Further investigation may elucidate the importance of these molecules, and whether the presence of resident fibroblasts is required or not. One final limitation for this study appears to be the use of cultured fibroblasts versus total lung cells in our scRNA-Seq experiments. Our data suggests that cells contributing to fibroblast populations in vivo change their phenotypes in response to being cultured on TC plastic. By looking at cells directly isolated from lung digests, a more accurate gene expression profile can be obtained for cells from bleomycin and saline-treated mice providing valuable insights into the mechanisms and processes that are occurring during fibrosis.

**Future Directions**

As discussed above, to gain a more accurate picture of the gene expression profiles, future studies could utilize scRNA-Seq to characterize total lung cells isolated

directly from bleomycin and saline-treated mice. In addition to this change, we will also use scRNA-Seq to evaluate total lung cells from bleomycin-treated mice that have received WCSD to understand what gene expression profiles have changed, and what potential gene pathways may be affected by treatment with WCSD. Future studies may also look at administering WCSD to bleomycin-treated mice at later time points after fibrosis has been initiated. Furthermore, two drugs that are FDA approved for the treatment of ILD, pirfenidone and nintedanib, could be evaluated for their effects on fibrocytes using similar research strategies, which could provide further insight into the mechanisms and pathways affected by these treatments thus leading to more targeted and effective therapies. In fact, one study by (Inomata, Kamio et al. 2014) has shown that pirfenidone was effective at reducing fibrocyte accumulation in the bleomycin-lung, and may further benefit from using the Vav1-Cre/mTmG mice to lineage trace the cells, and scRNA-Seq. Combinations of these therapeutics could also be evaluated in our model to see if there are any synergistic effects of these therapies.

## References


Aono, Y., et al. (2012). "Surfactant protein-D regulates effector cell function and fibrotic lung remodeling in response to bleomycin injury." American Journal of Respiratory and Critical Care Medicine **185**(5): 525-536.

Bhattacharyya, S., et al. (2016). "Tenascin-C drives persistence of organ fibrosis." Nature Communications **7**(1): 11703.

Borchers, A. T., et al. (2011). "Idiopathic pulmonary fibrosis-an epidemiological and pathological review." Clinical Reviews in Allergy and Immunology **40**(2): 117-134.

Borie, R., et al. (2013). "Detection of Alveolar Fibrocytes in Idiopathic Pulmonary Fibrosis and Systemic Sclerosis." PLoS One **8**(1): e53736.

Cao, H., et al. (2018). "Inhibition of Wnt/β-catenin signaling suppresses myofibroblast differentiation of lung resident mesenchymal stem cells and pulmonary fibrosis." Scientific Reports **8**(1).

Cheng, F., et al. (2016). "Vimentin coordinates fibroblast proliferation and keratinocyte differentiation in wound healing via TGF-β–Slug signaling." Proceedings of the National Academy of Sciences **113**(30): E4320-E4327.

Chueh, F.-S., et al. (2015). "Crude extract of Polygonum cuspidatum stimulates immune responses in normal mice by increasing the percentage of Mac-3-positive cells and enhancing macrophage phagocytic activity and natural killer cell cytotoxicity." Molecular Medicine Reports **11**(1): 127-132.

Daccord, C. and T. M. Maher (2016). "Recent advances in understanding idiopathic pulmonary fibrosis." F1000Research **5**: 1046.

Di Carlo, S. E. and L. Peduto (2018). "The perivascular origin of pathological fibroblasts." Journal of Clinical Investigation **128**(1): 54-63.

Dong, S. and R. Colin Hughes (1997). Glycoconjugate Journal **14**(2): 267-274.

Feng, M., et al. (2018). "Kupffer-derived matrix metalloproteinase-9 contributes to liver fibrosis resolution." International Journal of Biological Sciences **14**(9): 1033-1040.

Fischer, A. and R. Du Bois (2012). "Interstitial lung disease in connective tissue disorders." The Lancet **380**(9842): 689-698.

Foocharoen, C., et al. (2016). "Clinical characteristics of scleroderma overlap syndromes: comparisons with pure scleroderma." International Journal of Rheumatic Diseases **19**(9): 913-923.

Fujiwara, A., et al. (2012). "Correlation between circulating fibrocytes, and activity and progression of interstitial lung diseases." Respirology **17**(4): 693-698.

Galligan, C. L. and E. N. Fish (2012). "Circulating fibrocytes contribute to the pathogenesis of collagen antibody-induced arthritis." Arthritis and Rheumatism **64**(11): 3583-3593.

Gao, S. (2018). Data Analysis in Single-Cell Transcriptome Sequencing, Springer New York**:** 311-326.

Gendron, D. R., et al. (2017). "FTY720 promotes pulmonary fibrosis when administered during the remodelling phase following a bleomycin-induced lung injury." Pulmonary Pharmacology & Therapeutics **44**: 50-56.

Georgiades, P., et al. (2002). "vavCre Transgenic mice: A tool for mutagenesis in hematopoietic and endothelial lineages." genesis **34**(4): 251-256.

Ghavami, S., et al. (2018). "Autophagy and the unfolded protein response promote profibrotic effects of TGF-β1 in human lung fibroblasts." American Journal of Physiology-Lung Cellular and Molecular Physiology **314**(3): L493-L504.

Hagiwara, S., et al. (2007). "Antisense oligonucleotide inhibition of Heat Shock Protein (HSP) 47 improves bleomycin-induced pulmonary fibrosis in rats." Respiratory Research **8**(1): 37.

Harrison Jr, J. H. and J. S. Lazo (1987). "High dose continuous infusion of bleomycin in mice: A new model for drug-induced pulmonary fibrosis." Journal of Pharmacology and Experimental Therapeutics **243**(3): 1185-1194.

Haudek, S. B., et al. (2006). "Bone marrow-derived fibroblast precursors mediate ischemic cardiomyopathy in mice." Proceedings of the National Academy of Sciences of the United States of America **103**(48): 18284-18289.

Hinz, B., et al. (2012). "Recent Developments in Myofibroblast Biology." The American Journal of Pathology **180**(4): 1340-1355.

Inomata, M., et al. (2014). "Pirfenidone inhibits fibrocyte accumulation in the lungs in bleomycin-induced murine pulmonary fibrosis." Respiratory Research **15**(1): 16.

Ishida, Y. and K. Nagata (2011). Hsp47 as a collagen-specific molecular chaperone. Methods in Enzymology. **499:** 167-182.

Jang, H.-S., et al. (2014). "Recruitment and subsequent proliferation of bone marrow-derived cells in the postischemic kidney are important to the progression of fibrosis." American Journal of Physiology-Renal Physiology **306**(12): F1451-F1461.

Kakugawa, T., et al. (2013). "Serum heat shock protein 47 levels in patients with drug-induced lung disease." Respiratory Research **14**(1): 133.

Khalil, H., et al. (2019). "Cell-specific ablation of Hsp47 defines the collagen-producing cells in the injured heart." JCI Insight **4**(15).

Kleaveland, K. R., et al. (2014). "Fibrocytes are not an essential source of type I collagen during lung fibrosis." J Immunol **193**(10): 5229-5239.

Klecker, C. and L. S. Nair (2017). Matrix Chemistry Controlling Stem Cell Behavior. Biology and Engineering of Stem Cell Niches**:** 195-213.

Lee, R., et al. (2014). "Caveolin-1 regulates chemokine receptor 5-mediated contribution of bone marrow-derived cells to dermal fibrosis." Front Pharmacol **5**: 140.

Lee, R., et al. (2014). "Bleomycin delivery by osmotic minipump: similarity to human scleroderma interstitial lung disease." American Journal of Physiology-Lung Cellular and Molecular Physiology **306**(8): L736-L748.

Lee, R., et al. (2015). "Enhanced chemokine-receptor expression, function, and signaling in healthy African American and scleroderma-patient monocytes are regulated by caveolin-1." Fibrogenesis Tissue Repair **8**: 11.

Li, J., et al. (2007). "The Contribution of Bone Marrow-Derived Cells to the Development of Renal Interstitial Fibrosis." STEM CELLS **25**(3): 697-706.

Lin, C. M., et al. (2020). "Circulating fibrocytes traffic to the lung in murine acute lung injury and predict outcomes in human acute respiratory distress syndrome: a pilot study." Molecular Medicine **26**(1).

Masuda, H., et al. (1994). "Coexpression of the collagen-binding stress protein HSP47 gene and the α1 (I) and α1 (III) collagen genes in carbon tetrachloride-induced rat liver fibrosis." Journal of Clinical Investigation **94**(6): 2481-2488.

Mendez, M. G., et al. (2014). "Vimentin Enhances Cell Elastic Behavior and Protects against Compressive Stress." Biophysical Journal **107**(2): 314-323.

Miyamura, T., et al. (2020). "Small molecule inhibitor of HSP47 prevents pro-fibrotic mechanisms of fibroblasts in vitro." Biochemical and Biophysical Research Communications **530**(3): 561-565.

Moeller, A., et al. (2008). "The bleomycin animal model: A useful tool to investigate treatment options for idiopathic pulmonary fibrosis?" International Journal of Biochemistry and Cell Biology **40**(3): 362-382.

Mollmann, H., et al. (2006). "Bone marrow-derived cells contribute to infarct remodelling." Cardiovasc Res **71**(4): 661-671.

Moore-Morris, T., et al. (2014). "Resident fibroblast lineages mediate pressure overload-induced cardiac fibrosis." J Clin Invest **124**(7): 2921-2934.

Moore-Morris, T., et al. (2014). "Resident fibroblast lineages mediate pressure overload–induced cardiac fibrosis." Journal of Clinical Investigation **124**(7): 2921-2934.

Moore, B. B. and C. M. Hogaboam (2008). "Murine models of pulmonary fibrosis." American Journal of Physiology - Lung Cellular and Molecular Physiology **294**(2): L152-L160.

Mouratis, M. A. and V. Aidinis (2011). "Modeling pulmonary fibrosis with bleomycin." Current Opinion in Pulmonary Medicine **17**(5): 355-361.

Muñoz-Esquerre, M., et al. (2015). "Gene and Protein Expression of Fibronectin and Tenascin-C in Lung Samples from COPD Patients." Lung **193**(3): 335-343.

Muzumdar, M. D., et al. (2007). "A global double-fluorescent Cre reporter mouse." genesis **45**(9): 593-605.

Österreicher, C. H., et al. (2011). "Fibroblast-specific protein 1 identifies an inflammatory subpopulation of macrophages in the liver." Proceedings of the National Academy of Sciences **108**(1): 308-313.

Otsuka, M., et al. (2017). "Treatment of pulmonary fibrosis with siRNA against a collagen-specific chaperone HSP47 in vitamin A-coupled liposomes." Experimental Lung Research **43**(6-7): 271-282.

Pleasant-Jenkins, D., et al. (2017). "Reversal of maladaptive fibrosis and compromised ventricular function in the pressure overloaded heart by a caveolin-1 surrogate peptide." Lab Invest **97**(4): 370-382.

Quan, T. E., et al. (2004). "Circulating fibrocytes: collagen-secreting cells of the peripheral blood." The International Journal of Biochemistry & Cell Biology **36**(4): 598-606.

Reese, C., et al. (2013). "Differential regulation of cell functions by CSD peptide subdomains." Respir Res **14**(1): 90.

Reese, C., et al. (2014). "Caveolin-1 deficiency may predispose African Americans to systemic sclerosis-related interstitial lung disease." Arthritis Rheumatol **66**(7): 1909-1919.

Rockey, D. C., et al. (2015). "Fibrosis — A Common Pathway to Organ Injury and Failure." New England Journal of Medicine **372**(12): 1138-1149.

Roman, J., et al. (2004). "Nicotine and fibronectin expression in lung fibroblasts: implications for tobacco-related lung tissue remodeling." The FASEB Journal **18**(12): 1436-1438.

Ruiz-Villalba, A., et al. (2015). "Interacting resident epicardium-derived fibroblasts and recruited bone marrow cells form myocardial infarction scar." J Am Coll Cardiol **65**(19): 2057-2066.

Russell, T. M., et al. (2012). Flow Cytometric Identification of Fibrocytes in Scleroderma Lung Disease, Humana Press**:** 327-346.

Selman, M. and A. Pardo (2002). Respiratory Research **3**(1): 3.

Solomon, J. J., et al. (2013). "Scleroderma lung disease." European Respiratory Review **22**(127): 6-19.

Sun, H., et al. (2016). "Netrin-1 regulates fibrocyte accumulation in the decellularized fibrotic scleroderma lung microenvironment and in bleomycin induced pulmonary fibrosis." Arthritis & Rheumatology: n/a-n/a.

Sunamoto, M., et al. (1998). "Expression of heat shock protein 47 is increased in remnant kidney and correlates with disease progression." International Journal of Experimental Pathology **79**(3): 133-140.

Swaney, J., et al. (2010). "A novel, orally active LPA1 receptor antagonist inhibits lung fibrosis in the mouse bleomycin model." British Journal of Pharmacology **160**(7): 1699-1713.

Tang, N., et al. (2014). "Lysophosphatidic acid accelerates lung fibrosis by inducing differentiation of mesenchymal stem cells into myofibroblasts." Journal of Cellular and Molecular Medicine **18**(1): 156-169.

Tourkina, E., et al. (2008). "Antifibrotic properties of caveolin-1 scaffolding domain in vitro and in vivo." American Journal of Physiology - Lung Cellular and Molecular Physiology **294**(5): L843-L861.

van Amerongen, M. J., et al. (2008). "Bone marrow-derived myofibroblasts contribute functionally to scar formation after myocardial infarction." J Pathol **214**(3): 377-386.

Visconti, R. P. and R. R. Markwald (2006). "Recruitment of new cells into the postnatal heart: potential modification of phenotype by periostin." Ann N Y Acad Sci **1080**: 19-33.

Vonk Noordegraaf, A., et al. (2016). "Pulmonary hypertension." European Respiratory Review **25**(139): 4-11.

Wang, H., et al. (2019). "MMP-9-positive neutrophils are essential for establishing profibrotic microenvironment in the obstructed kidney of UUO mice." Acta Physiologica **227**(2).

Wang, Q., et al. (2019). "Dynamic features of liver fibrogenesis and fibrosis resolution in the absence of matrix metalloproteinase-9." Molecular Medicine Reports.

Wang, S., et al. (2016). "TGF-β/Smad3 signalling regulates the transition of bone marrow-derived macrophages into myofibroblasts during tissue fibrosis." Oncotarget **7**(8): 8809-8822.

Wang, Z. L. (2009). "Advances in understanding of idiopathic pulmonary fibrosis." Chinese Medical Journal **122**(7): 844-857.

Wollin, L., et al. (2019). "Potential of nintedanib in treatment of progressive fibrosing interstitial lung diseases." European Respiratory Journal **54**(3): 1900161.

Wynn, T. A. (2004). "Fibrotic disease and the TH1/TH2 paradigm." Nature Reviews Immunology **4**(8): 583-594.

Xie, T., et al. (2018). "Single-Cell Deconvolution of Fibroblast Heterogeneity in Mouse Pulmonary Fibrosis." Cell Reports **22**(13): 3625-3640.

Yang, L., et al. (2002). "Peripheral blood fibrocytes from burn patients: Identification and quantification of fibrocytes in adherent cells cultured from peripheral blood mononuclear cells." Laboratory Investigation **82**(9): 1183-1192.

Yata, Y., et al. (2003). "DNase I-hypersensitive sites enhance alpha1(I) collagen gene expression in hepatic stellate cells." Hepatology **37**(2): 267-276.

Zhao, Y., et al. (2019). "Pharmacoproteomics reveal novel protective activity of bromodomain containing 4 inhibitors on vascular homeostasis in TLR3-mediated airway remodeling." Journal of Proteomics **205**: 103415.